Received: 30 April 2020 | Revised: 23 May 2020 | Accepted: 2 June 2020

DOI: 10.1002/eom2.12038

REVIEW

EcoMat FUNCTIONAL MATERIALS FOR GREEN ENERGY AND ENVIRONMENT WILEY

Potassium-sulfur batteries: Status and perspectives

Xinyu Zhao[1,2] | Yan Lu[2] | Zhengfang Qian[1] | Renheng Wang[1] | Zaiping Guo[2]

[1]College of Physics and Optoelectronic Engineering, Shenzhen University, Shenzhen, China

[2]School of Mechanical, Materials, Mechatronic and Biomedical Engineering, Australian Institute for Innovative Materials, Institute for Superconducting & Electronic Materials, University of Wollongong, New South Wales, Australia

Correspondence
Yan Lu and Zaiping Guo, School of Mechanical, Materials, Mechatronic and Biomedical Engineering, Australian Institute for Innovative Materials, Institute for Superconducting & Electronic Materials, University of Wollongong, New South Wales 2522, Australia.
Email: yanl@uow.edu.au (Y. L.) and zguo@uow.edu.au (Z. G.)

Renheng Wang, College of Physics and Optoelectronic Engineering, Shenzhen University, Shenzhen 518060, China.
Email: wangrh@szu.edu.cn (R. W.)

Funding information
Australian Research Council, Grant/Award Numbers: DE190100082, DP200101862, LP160101629; China Postdoctoral Science Foundation, Grant/Award Number: 2019M663047; National Natural Science Foundation of China, Grant/Award Number: 51804199; Natural Science Foundation of Guangdong Province, Grant/Award Number: 2019A1515012111; Science and Technology Innovation Commission of Shenzhen, Grant/Award Numbers: 20180123, JCYJ20190808173815205; Shenzhen Science and Technology Program, Grant/Award Number: KQTD20180412181422399

Abstract

This review article aims to provide insight into the research status of the potassium-sulfur (K-S) system, feature the challenges facing this technology, and present possible research directions for the realization of its practical applications. We begin with an introduction to the fundamental electrochemistry of K-S batteries and emphasize the distinctions between K-S technology and the well-established lithium-sulfur (Li-S) system. Then, we focus on the development of the materials involved in K-S batteries in terms of cathodes, K anodes, and various electrolyte systems. Finally, we provide several possible research directions to make the K-S system a reality, with the emphasis, from our point of view, on the attempts to construct practical parameters for K-S batteries by adopting the critical metrics of the current Li-S system.

KEYWORDS

electrochemistry of sulfur, potassium anode protection, potassium polysulfides, potassium-sulfur batteries, shuttle effect

1 | INTRODUCTION

Electrochemical energy storage devices play vital roles in combating today's energy crisis and environmental issues by enabling efficient utilization of renewable forms of energy, such as solar and wind, which require high energy density, long cycle life, low cost, and high safety.[1-4] As a great success of modern energy-storage technology, commercial Li-ion batteries (LIBs) can reach a gravimetric energy density of around 200 W h kg^{-1} and have enabled transformative advances in many technologies, from portable electronics to the electrification of transportation.[5-7] The ceiling capacity of commercialized LIBs will be soon reached, however, due to the limitations of their insertion chemistry.[8] Thus, exploring new battery chemistries that can generate even higher energy densities for longer usage time of electronics and higher energy-storage capabilities than current lithium ion batteries is an urgent need for powering our future society.

Metal-sulfur batteries based on sulfur chemistry are intriguing alternatives to succeed the current dominant LIBs and support our fast-expanding energy demands.[6,9-11] Among them, research on lithium-sulfur batteries has achieved remarkable progress over the past few decades.[12-14] Having sulfur as the cathode material provides a theoretical energy density of 2600 Wh kg^{-1} or 2800 Wh L^{-1} on coupling with lithium-metal anode, far exceeding those of state-of-the-art LIBs.[15-17] In addition, the commercial potential of the lithium-sulfur (Li-S) system has been demonstrated in some niche applications. For example, some companies have announced prototype Li-S batteries operating in an unmanned system, electric bicycles, and test applications, while more are rushing to develop sulfur batteries. Despite extensive progress, Li-S based technology is unable to meet large-scale energy storage demands because of the limited abundance of Li resources and its high price.[18] On the other hand, for grid-related applications, where scale and cost are as important as performance, the abundant low cost sodium-sulfur (Na-S) battery system is preferable. In reality, the molten-salt type high-temperature Na-S system is well established and has been used to support stationary energy-storage systems for several decades.[4,19-22] Nevertheless, the highly dangerous nature of molten Na and S in the high-temperature Na-S system makes it unacceptable in some applications (such as transportations) owing to the safety concerns.[23-25] As a result, room-temperature Na-S batteries that adopt the advantages of the high-temperature Na-S system at low-temperature under safer operating conditions have aroused the enthusiasm of researchers.[26-30] Similar to Li-S batteries, however, the practical application of room-temperature Na-S batteries faces the challenges of low electrochemical utilization, reversibility, and efficiency.[26,31-33] Additional challenges, such as the lack of favorable liquid electrolyte for the complicated reaction of sulfur and sodium, also need to be overcome before it becomes a reality.[2,34,35]

Being the next alkaline metal to sodium, potassium, with some unique advantages over lithium and sodium, has drawn substantial attention from the scientific community as a future battery system of interest. Potassium-sulfur (K-S) batteries benefit from the low standard reduction potential of potassium compared to the standard hydrogen electrode (SHE) potential (−2.93 V vs E^0) (Figure 1A), and offer high specific capacity and energy density.[8,34] In addition, the low cost of raw materials (ie, K_2CO_3) owing to the abundance potassium (seventh most abundant material in Earth's crust),[44,45] makes it particularly promising for large-scale applications, such as electric vehicles and grid-related energy storage. The electrochemical advantages of K in organic electrolytes, for instance, the weaker Lewis acidity of K^+ than Li^+ and Na^+ results in a smaller Stokes' radius (3.6 Å vs 4.8 and 4.6 Å) in carbonate solvents (Figure 1A),[46] endowing K^+ with the highest ion mobility, ion conductivity, and ion transport number of the three ions.[17] Also, theoretical calculations and experiments have demonstrated that the K^+/K redox couple exhibits the lowest reduction potential in organic solvents as compared to Li^+/Li and Na^+/Na,[44,46,47] implying that a relatively high voltage for a full battery may be possible. Furthermore, enhanced electrolyte/electrode interfacial diffusion capacity of K^+ is expected due to its low desolvation energy, which has enabled the insertion of large-radius K^+ in graphite.[48,49] Most importantly, the K-S battery offers a high theoretical gravimetric energy density of 914 Wh kg^{-1},[50] much higher than that for commercial LIBs, which is the key motivation for in-depth investigations into this system.

Nevertheless, the research on the K-S system is still in its infancy, and a number of challenges have been encountered on the road to its development. For example, as in the Li-S and Na-S systems, the insulating nature of sulfur/polysulfide, both electronically and ionically, and the dissolution of polysulfide intermediates, result in poor utilization of the active material, leading to severe capacity decay during cycling. For example, in a K-S battery using sulfur as the cathode active material, although a decent capacity of 600 mA h g^{-1} was maintained after 50 cycles at 0.1 C by virtue of a designed functional separator, the capacity loss due to the insufficient use of active material was still as high as 50%.[51] This implies that there is still

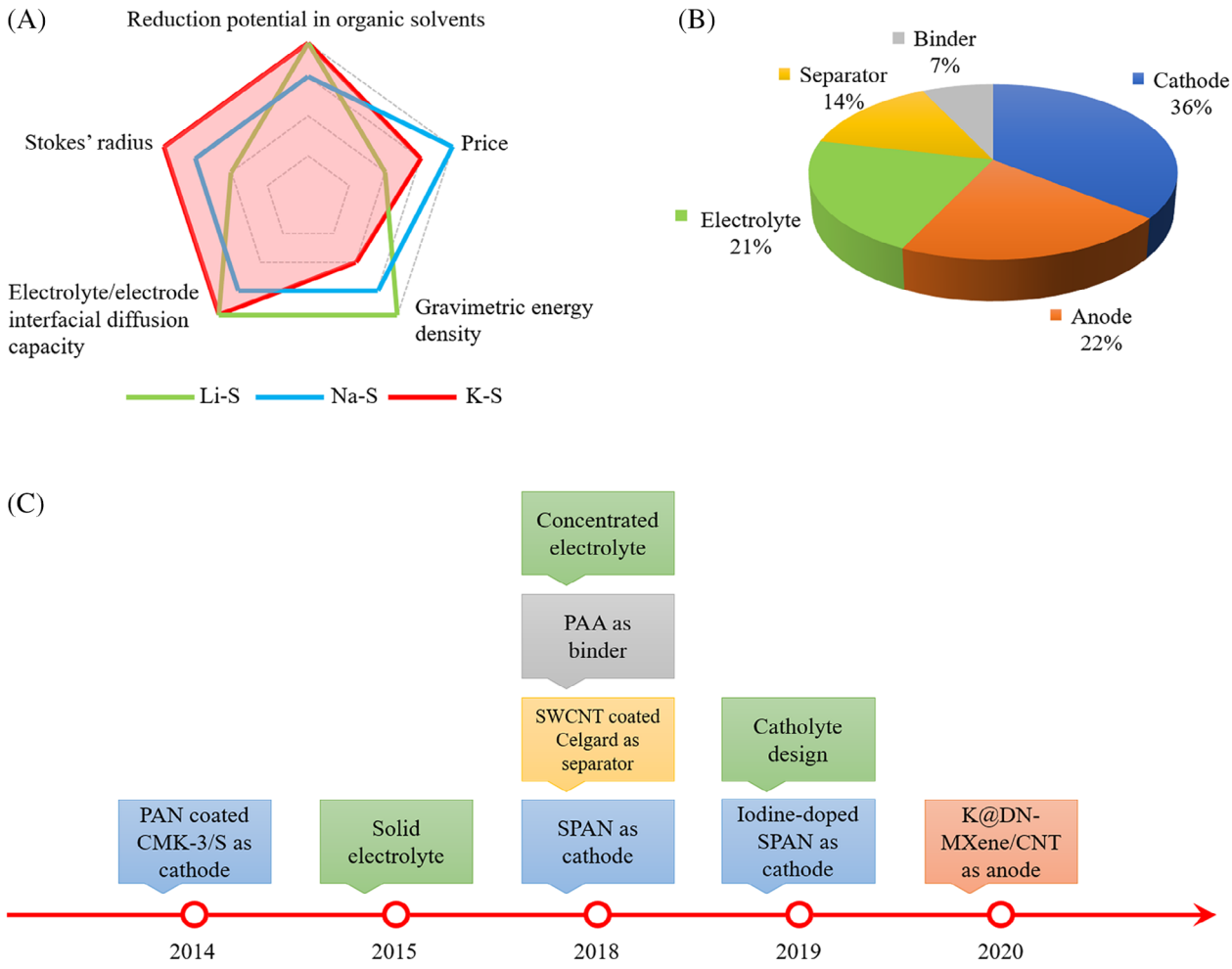

FIGURE 1 A, Comparison of the properties and performances of Li-S, Na-S and K-S batteries. B, Percentage of numbers of publications on different K-S battery topics. C, Strategies developed to improve the electrochemical performance of K-S batteries each year since the invention of the first K-S battery in 2014[8,36-43]

a long way to go for K-S to achieve high energy density suitable for practical applications. More challenging than for Li-S and Na-S, an even larger volume change will occur upon potassiation of sulfur-based cathodes due to the large size of potassium ion, leading to severe pulverization of the active material during cycling. Another thorny problem of K-S is the formation of K dendrites and the unstable solid electrolyte interphase (SEI), causing safety concerns and poor Coulombic efficiency (CE), which need to be addressed to promote the development of the K-S battery.[52] With a clear awareness of those difficulties, great efforts are required, and achieving an in-depth understanding is indispensable in this area. Figure 1B summarizes research preferences on different components of K-S battery from published research articles where cathode, anode, and electrolyte are the most addressed topics in K-S research articles. Figure 1C shows a timeline of strategies developed to improve the electrochemical performance of K-S batteries each year since the invention of the first room-temperature K-S battery in 2014. With evidence of the increasing interest in the K-S battery and the feasible adoption of knowledge accumulated on Li-S, Na-S, and potassium-ion batteries (PIBs), we believe that both our basic understanding and the performance of K-S technology could be improved tremendously in the near future.

This review aims to provide a comprehensive overview of the research status of K-S batteries. First, we start with some insight into the electrochemistry of K-S batteries. Meanwhile, an electrochemical mechanism comparison of Li-S, Na-S, and K-S technologies will be presented, and challenges for K-S system will be highlighted. Then, we examine the materials involved in K-S batteries, mainly focusing on the design strategies and improvements for sulfur/

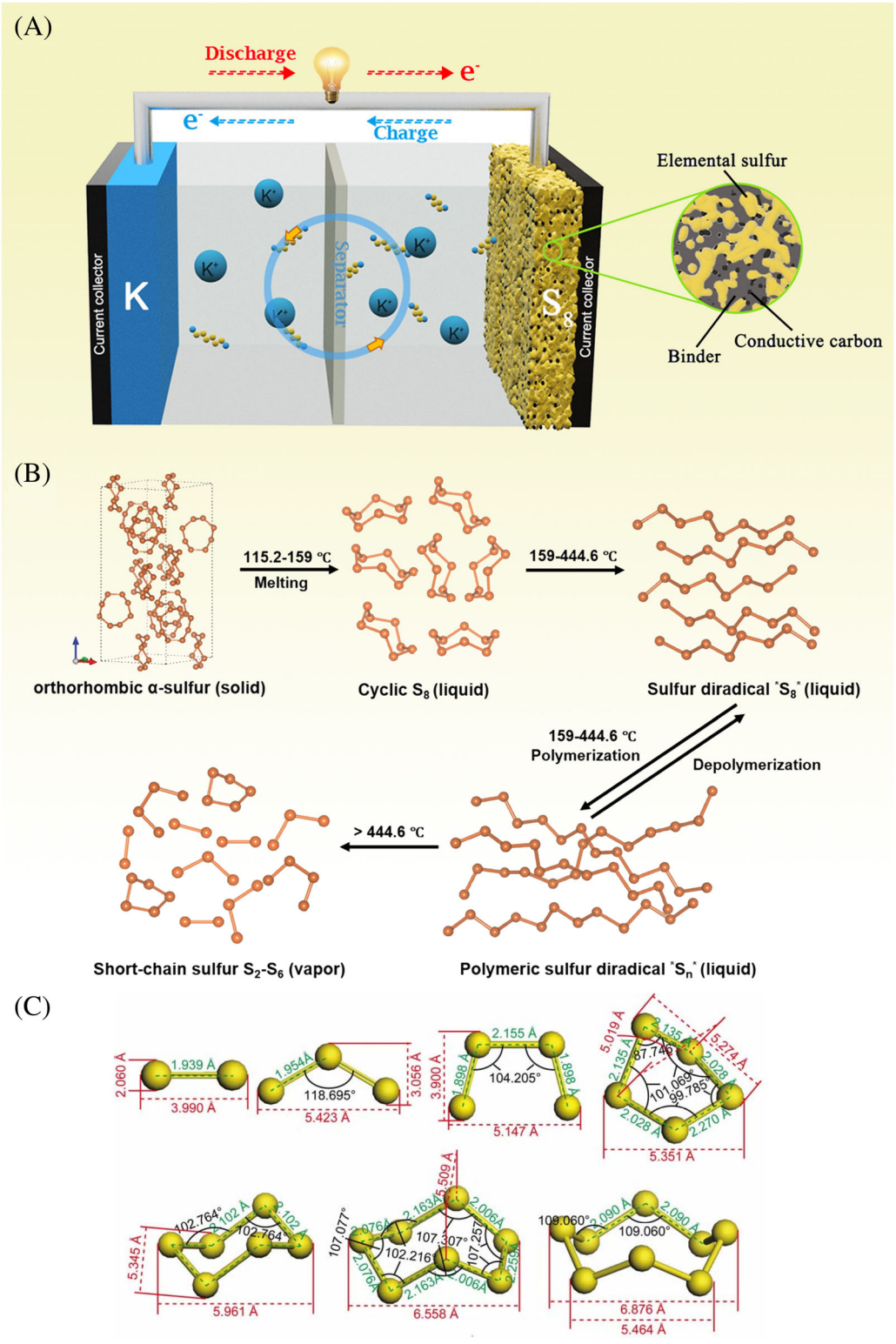

FIGURE 2 A, Schematic illustration of the configuration of a K-S battery. B, Structur transformation of elemental sulfur at various temperatures. Reproduced with permission. Copyright 2020, Royal Society of Chemistry.[53] C, The sulfur allotropes from S_2 to S_8 based on density functional theory (DFT) calculations. Reproduced with permission. Copyright 2012, American Chemical Society[54]

polysulfide-based conversion cathodes, K anodes, and various electrolyte systems. Representative examples will be presented, and the progress will be discussed. Finally, our views on the existing challenges and future research directions of advanced K-S batteries will be shared.

2 | ELECTROCHEMISTRY AND CHALLENGES OF POTASSIUM-SULFUR BATTERIES

2.1 | Electrochemistry of potassium-sulfur batteries

A typical configuration for a K-S battery consists of a K metal anode, a sulfur composite cathode, a separator, and an organic electrolyte (Figure 2A). The charge/discharge process involves reversible plating/stripping of the K metal at the anode and a reversible anion redox reaction of sulfur at the cathode, while K^+ and electrons travel through the electrolyte and the external circuit, respectively. Notably, owing to the insulating nature of sulfur, the cathode is commonly constructed of sulfur, conductive carbon, and binder. The electrochemical reactions for a metal (M)-sulfur battery with the transfer of a number of (n) electrons are generally expressed as

$$\text{Anode}: M \leftrightarrow M^+ + e^- \quad (1)$$

$$\text{Cathode}: S_n + 2nM^+ + 2ne^- \leftrightarrow nM_2S \ (1 \le n \le 8) \quad (2)$$

On the anode side, K metal undergoes a redox reaction with the transfer of one electron, similar to that in PIBs,[7,55-57] while on the cathode side, the initial state of sulfur is complex, because it may contain a number of sulfur allotropes. Theoretically, with a two-electron transfer, all the sulfur can give a maximum capacity of 1675 mAh g^{-1} regardless of the allotropes. Nevertheless, the reaction pathway of K-S varies according to the different forms of allotropes. Thus, it is important to acquire a basic understanding of sulfur chemistry, as will be discussed.

It is noteworthy that the initial states of sulfur in the cathode determine the detailed mechanism of the electrochemical reaction of metal-sulfur batteries. Generally, it contains two categories: cyclo-octasulfur (S_8)/polymeric sulfur and short-chain sulfur. Different types of sulfur allotropes can be synthesized via different heat-treatments as indicated in Figure 2B. In particular, cyclo-octasulfur, also known as α-sulfur, has a stable orthorhombic solid state at room temperature. It starts to melt when the temperature reaches 115.2°C (melting point) and reaches the minimum viscosity of molten sulfur at about 159°C, making it suitable for impregnation into a matrix material. This leads to the successful fabrication of sulfur composites at 155°C, such as the first reported CMK-3/sulfur composite cathode for the K-S battery.[36] When the heating temperature increases over 159°C but is lower than 444.6°C (boiling point), highly reactive diradical polymeric sulfur chains form and can be stabilized via copolymerization with many functional groups, resulting in the formation of polymeric sulfur and also various sulfur-rich copolymers with embedded $-S_n-$ moieties. Generally, a temperature of 185°C is often used for promoting efficient ring opening polymerization during the sulfur copolymerization process.[58] There have been several reports studying polymeric sulfur in K-S batteries, and it is believed that more will be published in this area as there are numerous related works on Li-S batteries,[59] which would provide sufficient inspiration. When it is heated over 444.6°C (boiling point), sulfur will be dissociated into short chains (S_2-S_6). For instance, small sulfur molecules (S_n, $n \le 3$) embedded in microporous carbon composite cathode have been demonstrated in K-S batteries, which were prepared by a high-temperature heat treatment of bulk S_8 at 600°C.[60] Thus, it is possible to tune the initial form of sulfur in composite cathodes to choose the most favorable reaction pathway for high-performance and low cost K-S batteries.

Even though the cathode electrochemistry is very complex, the general reduction pathways of sulfur allotropes (S_2-S_8), with structures that are predicted using density functional theory (DFT) calculations in Figure 2C, are recognized for metal-sulfur batteries. In the case of the ring-shaped high-order S_n ($5 \le n \le 8$), they are sequentially reduced to long-chain polysulfides (S_n^{2-}, $5 \le n \le 8$), then short-chain polysulfides (S_n^{2-}, $2 \le n \le 4$), and finally, the end member sulfide (S^{2-}). In the case of the low-order sulfur allotropes, which possess chain-shaped structures, their reductions bypass the formation of long-chain polysulfides to reach the end product sulfide (S^{2-}). An overview of the reactions and basic energy parameters for different types of alkali metal-based sulfur batteries are summarized in Table 1.

The K-S battery undergoes a qualitatively analogous process to those of Li-S[53] and Na-S,[61] but with less distinct sloping plateaus, lower overall redox voltages, and a larger charge-discharge hysteresis (Figure 3A-C). Notably, the discharge plateaus of K-S are relatively short and sloping, compared to the long and flat plateaus of Li-S, therefore a considerable proportion of the discharge capacity in K-S comes from the sloping area instead of the platform area. The reason for this phenomenon is complexed, and larger voltage polarization in K-S battery could be one of them. Given the fact that the exact intermediate K_2S_n phase sequence is yet to be discovered, it is hard to say that K-S has similar polysulfide intermediates sequence to those for Li-S and Na-S. Even worse, the composition of the discharge product for K-S is still debatable. It seems to vary with the applied cut-off voltage (COV). As a result, some are reported to be K_2S (COV $\le$ 1 V),[51,60] while some are identified as K_2S_3

TABLE 1 Fundamental properties of metal-sulfur systems (potassium vs sodium and lithium)

Alkali metals	Potassium	Sodium	Lithium
Reactions	$2K + \frac{1}{8}S_8 \Leftrightarrow K_2S$	$2Na + \frac{1}{8}S_8 \Leftrightarrow Na_2S$	$2Li + \frac{1}{8}S_8 \Leftrightarrow Li_2S$
Gibbs free energies[a] [ΔG, kJ mol^{-1}]	−362.73	−357.77	−432.57
Theoretical cell voltage[a] [E^0, V]	1.88	1.85	2.24
Gravimetric energy density[a] [Wh kg^{-1}]	914	1273	2615
Volumetric energy density[a] [Wh L^{-1}]	1590	2363	4289
Volume expansion[a] [ΔV, %]	309	171	80
Stable phases at room temperature	K_2S, K_2S_2, K_2S_3, K_2S_4, K_2S_5, K_2S_6	Na_2S, Na_2S_2, Na_2S_4, Na_2S_5	Li_2S

[a]Values obtained from Reference 50.

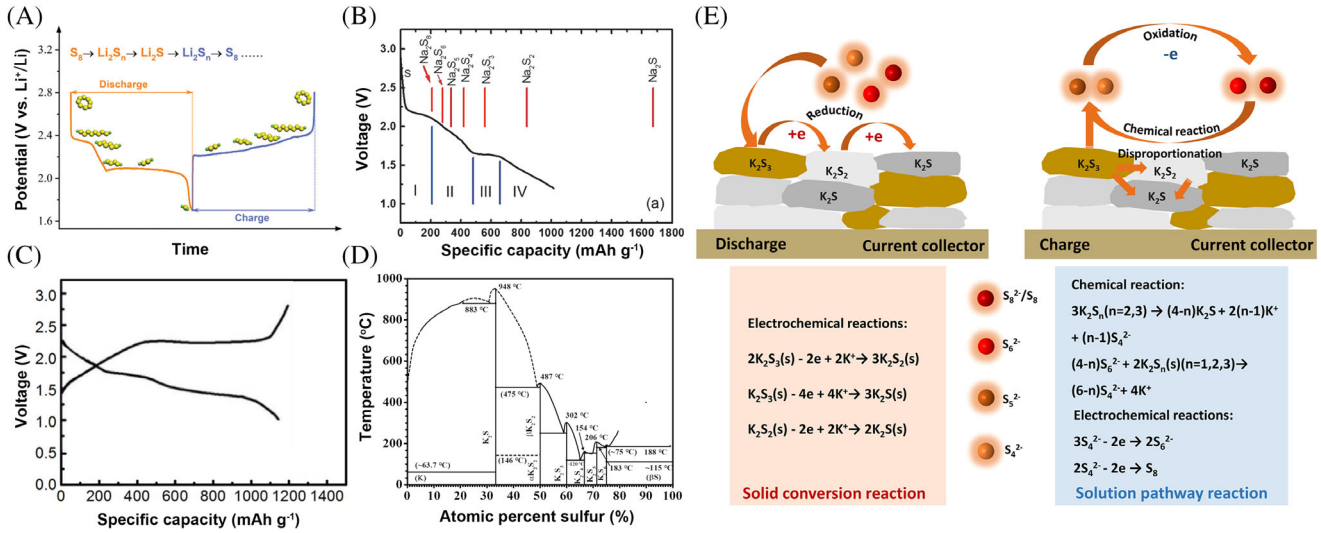

FIGURE 3 A, Typical voltage profiles illustrating the sulfur conversion reactions for a Li-S battery, Reproduced with permission. Copyright 2020, Royal Society of Chemistry.[53] B, Typical voltage profile for a Na-S battery. Reproduced with permission. Copyright 2014, Wiley-VCH.[61] C, Representative voltage profiles for a K-S battery. Reproduced with permission. Copyright 2018, Elsevier.[51] D, An assessed K-S phase diagram. Reproduced with permission. Copyright 2019, American Chemical Society.[60] E, Schematic illustration of the reaction mechanism for K-S batteries during cycling: the solid conversion reaction in discharging and the solution pathway reaction in charging. Reproduced with permission. Copyright 2018, American Chemical Society[62]

(COV > 1 V).[62] Theoretical calculation using DFT shows that K_2S, with the lowest formation energy, is the most thermodynamically stable phase. As K_2S_2 has a higher formation energy than K_2S_3 and K_2S, it is a less thermodynamically stable form. Therefore, K_2S_2 phase tends to disproportate to form more stable phases of K_2S_3 and K_2S.[60] Because the final discharge product determines the number of electrons involved in the reaction, it is highly related to the theoretical capacities that can be reached, as shown in Table 2, such as 558 mAh g^{-1} for K_2S_3 vs 1675 mAh g^{-1} for K_2S. Nevertheless, for the currently reported K-S batteries, maximum capacities are in the range of 500 to 1140 mAh g^{-1}, showing a large gap between the theoretical capacities and the reported ones. Thus, determining the origin of this discrepancy and how it relates to the intermediate phase sequence is essential for achieving high energy density with K-S technology.

Although we are still at a very preliminary stage, some efforts have been made to find the electrochemical mechanisms related to the key intermediates in K-S batteries, that is, K_2S_3, K_2S_2, and K_2S. According to the K-S phase diagram (Figure 3D), a series of phases of K_2S_n ($n = 1, 2, 3, 4, 5, 6$) are stable at room temperature, which is different from what occurs in the Li-S and Na-S systems.[60] This unique property makes it possible to investigate the mechanism of K-S intermediates using pure-phase solid polysulfides. By taking advantage of this, two crucial intermediates of potassium polysulfide (K_2S_3 and K_2S_2) were synthesized and their electrochemical pathways in the K-S battery were revealed.[62] As depicted in Figure 3E, during the discharge process, K_2S_2 and K_2S_3

TABLE 2 Parameters for the K-S battery based on polysulfide species

Material	Number of electrons involved in charge transfer	Theoretical capacity, mAh g^{-1} (cumulative)	Solubility in DME	Solubility in DEGDME
K_2S_8	1/4 e^-	209.375	Soluble	N/A
K_2S_6	1/3 e^-	279.167	Soluble	Soluble
K_2S_5	2/5 e^-	335.000	Soluble	Soluble
K_2S_4	1/2 e^-	418.750	Soluble	Insoluble
K_2S_3	2/3 e^-	558.333	Slightly soluble (71.4 ± 18.0 mg $[100\ g]^{-1}$)	Insoluble
K_2S_2	1 e^-	837.500	Slightly soluble (12.6 ± 4.7 mg $[100\ g]^{-1}$)	Insoluble
K_2S	2 e^-	1675.000	Insoluble	Insoluble

Abbreviations: DEGDME, diethylene glycol dimethyl ether; DME, dimethoxyethane.

can be further reduced to K_2S via a solid-phase conversion dominated reaction. Due to the insolubility of K_2S_2 and K_2S_3 in electrolyte, however, the accumulation of them on the cathode causes sluggish kinetics and terminates the discharge reaction with high overpotential. Therefore, to promote this reaction, efficient catalysts that catalyze the reduction reaction are promising to improve the reaction kinetics and facilitate the formation of K_2S. The charge process, however, is controlled by the solution pathway coupling the chemical and electrochemical reactions, resulting in an asymmetry with respect to the discharge process. During this, soluble species (S_4^{2-}, S_5^{2-}, and S_6^{2-}) generated from disproportionation reaction are changed to high-order species (S_6^{2-}, S_8^{2-}, and S_8), and the insoluble species are transformed into S_4^{2-} by chemical reaction. Notably, the K_2S cannot be oxidized through the solution electrochemical pathway and remains inactive, leading to the formation of "dead polysulfide" that fails to contribute to overall capacity. This mechanism investigation would accelerate progress on understanding the detailed reaction pathways related to the complex polysulfides inside the K-S battery.

2.2 | Challenges of potassium-sulfur batteries

Being at an early development stage, the K-S system is facing a series of challenges that must be overcome before it becomes a reality (Figure 4). Similar challenges also exist in the Li-S and Na-S systems, but some are exclusive for to the K-S batteries. All of them are critical and need to be overcome to realize a practical K-S battery with high energy density and long cycling life.

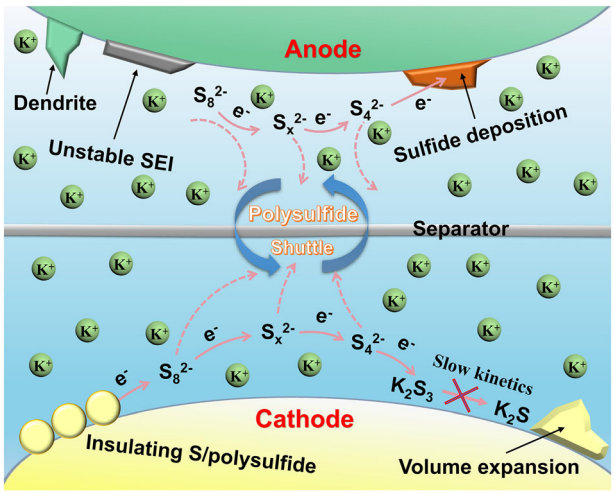

FIGURE 4 Challenges of potassium-sulfur batteries

2.2.1 | Insulating nature of sulfur and potassium polysulfide/sulfide

The issue of the low conductivity of sulfur and polysulfide/sulfide is ubiquitous for metal-sulfur batteries, which results in poor utilization of the active material. In addition, their precipitation on the surface of cathode/anode during cycling causes electrode passivation, limiting the capacity that can practically be achieved.

2.2.2 | Sluggish reduction kinetics of K_2S_3 to K_2S

K-S batteries usually operate between S and K_2S_3 at room temperature owing to the higher thermodynamic stability of K_2S_3 (Gibbs energy of formation at 25°C, ΔG_f^0

$= -528\,kJ\,mol^{-1}$) compared to K_2S ($\Delta G_f^0 = -410\,kJ\,mol^{-1}$).[37,63,64] The incomplete reduction of sulfur causes a dramatic decrease in the theoretical capacity from 1675 mAh g^{-1} (2 e^- transfer for K_2S) to 558 mAh g^{-1} (2/3 e^-) (Table 2), which is really harmful for practically achieving high capacity. In addition, a large overpotential is required for further reduction of the energetically stable K_2S_3, thus resulting in a low average operating voltage. The combination of low achievable capacity and reduced operating voltage impede the attainment of high energy density for the K-S system.

2.2.3 | Large volumetric expansion of sulfur during potassiation

Because of the large size of potassium ions, sulfur undergoes a large volumetric expansion of 309% upon full potassiation to potassium sulfide, which is much larger than those for Li (80%) and Na (171%) (Table 1). This expansion can cause pulverization and structural damage at the electrode level, which is undesirable for long cycling life.

2.2.4 | Polysulfide shuttle effect

Akin to Li-S batteries, the shuttle effect is a key challenge for K-S batteries to achieve high energy density and long cycling life. It is caused by the dissolution and diffusion of polysulfide intermediates. Parasitic reactions take place when those redox active species diffuse to the anode, where they are reduced chemically (instead of electrochemically) to lower-order polysulfides or sulfides, causing the loss of active materials as well as the passivation of anode materials. They can also diffuse back to the sulfur cathode to be re-oxidized.[65] Thus, the shuttle effect is essentially an internal short circuit, leading to self-discharging and low CE during charge/discharge cycling.[12]

2.2.5 | Unstable solid electrolyte interphase

Potassium is highly reactive and thus inevitably reacts with the electrolyte to form an SEI layer on the surface. In most cases, the SEI is unstable and fails to passivate the potassium metal surface, inducing continuous side reactions with the electrolyte during cycling. This undesirable consumption of potassium metal and electrolyte leads to poor reversibility and low CE during repeated plating and stripping.

2.2.6 | Dendrite growth of potassium metal

The uneven plating and stripping of potassium would lead to the growth of potassium dendrites, which accompany the continuous breaking and reforming of the SEI, further consuming the potassium metal and electrolyte. Moreover, the dendrites might penetrate the separator and lead to internal short circuits, inducing serious safety concerns.

Considerable efforts have been made to address the challenges mentioned above, in order to enhance the kinetics of the S-based cathode, alleviate the shuttle effect, and build a stable/safe potassium anode. Approaches focusing on the construction of novel cathode architectures, the protection of anode materials, and optimization of the electrolyte have been explored, and notable progress has been achieved. Representative examples of these approaches will be discussed in the following sections.

3 | MATERIALS INVOLVED IN POTASSIUM-SULFUR BATTERIES

Similar to the structure of lithium-sulfur and sodium-sulfur batteries, potassium-sulfur batteries are composed of a sulfur positive electrode, a K metal negative electrode, a K ion containing electrolyte, and a separator (Figure 2A). Each component has its unique features and challenges. For example, the sulfur cathode has an intrinsic insulating issue, polysulfide migration to the electrolyte, and the shuttling issue, while K metal anode has the dendrite issue. The specific challenges and possible solutions for the cathode, anode, and electrolyte are included in this section. To date, numerous exquisite material design and structure engineering approaches have been proposed for single components or the whole K-S battery. Table 3 lists the design strategies and electrochemical performance from recent K-S battery research work. Many of these strategies are inherited from the knowledge obtained from Li-S and Na-S batteries. Due to the unique challenge arising from the K anode (eg, larger ion radius and higher electrochemical activity), new strategies designed for the K-S battery are still needed. Furthermore, in order to improve the full range of K-S battery performance and promote practicality, several of these strategies could be coupled, and new challenges that may arise from such cooperation need to be considered in future designs.

TABLE 3 The components and electrochemical performance of current state-of-the-art K-S batteries

Strategy	Cathode [binder]	Anode [separator]	Electrolyte	Sulfur content [S loading ($mg\ cm^{-2}$)]	Capacity mAh g_{sulfur}^{-1} [initial CE]	Capacity retention (%) [number of cycles]	Voltage window (V)	Ref.
Cathode design	Polyacrylonitrile (PAN) coated CMK-3/sulfur [PTFE]	K metal [glass fiber]	1 M $KClO_4$ in TEGDME	40.8 wt% [Not Rep.]	512.7 [99%]	39.4% [50]	1.2-2.4	36
Cathode design	Sulfurized carbonized polyacrylonitrile (SPAN) [PVDF]	K metal [glass fiber]	0.8 M KPF_6 in EC/DEC	38 wt% [≈0.38]	710 [53%]	54% [100]	0.8-2.9	38
Cathode design	Iodine-doped sulfurized polyacrylonitrile [PVDF]	K metal [glass fiber]	0.8 M KPF_6 in EC/DEC	17.7 wt% [≈0.18]	1010 [61.4%]	53.7% [180]	0.8-2.9	66
Cathode design	SPAN [CMC]	K metal [glass fiber]	1 M KOTF in EC/DEC	39.3 wt% [0.4-0.6]	873.9 [72.9%]	86.3% [300]	0.8-3.0	67
Cathode design	Microporous carbon/ small molecule sulfur composites [CMC]	K metal [polypropylene membrane]	0.8 M KPF6 in EC/DEC	20 wt% [<1]	1198.3 [61.9%]	72.5% [150]	0.5-3.0	60
Cathode design and high safety anode	K_2S_x/3D-CNT film [not rep.]	K-impregnated hard carbon [glass fiber]	0.5 M KTFSI in DEGDME	Not rep. [0.44 mg per cell]	≈400 [88.9%]	94% [20]	1.2-2.4	68
Cathode and binder design	SPAN [10 wt% PAA with PVDF]	K metal [glass fiber]	0.5 M KPF6 in EC/DMC	45.5 wt% [0.8]	1050 [46.7%]	95% [100]	0.1-3.0	39
Cathode and separator design	Carbon nanofiber paper/ sulfur composites [binder-free]	K metal [SWCNT coated Celgard]	1 M KOTF in TEGDME	50 wt% [≈1]	1140 [95%]	52.6% [50]	1.0-2.8	51
Cathode and separator design	CNT/sulfur composites [PVDF]	K metal [Nafion-K+ Celgard]	0.6 M KFSI in DME	70 wt% [0.48]	720 [52.7%]	25.6% [5]	1.2-3.0	62
Anode design	SPAN [PVDF]	K@DN-MXene/CNT anode [glass fiber]	0.8 M KPF_6 in EC/DEC	Not rep. [1.2]	638 [not rep.]	36% [500]	0.8-2.8	41
Anode and catholyte design	Sulfur/vulcan carbon (S_8/VC) [PVDF]	1.0 M BpK in DME [quartz fiber]	polymer-laminated K-β″-Al_2O_3 + catholyte (0.3 M $Cu(TFS)_2$, 0.1 M KTFS in Me-Im)	Not rep. [1-1.2]	922 [not rep.]	84% [200]	1.0-3.0	37

(Continues)

TABLE 3 (Continued)

Strategy	Cathode [binder]	Anode [separator]	Electrolyte	Sulfur content [S loading (mg cm^{-2})]	Capacity mAh g_{sulfur}^{-1} [initial CE]	Capacity retention (%) [number of cycles]	Voltage window (V)	Ref.
Concentrated electrolyte	CMK-3/sulfur composites [PVDF]	K metal [glass fiber]	5 M KTFSI in DEGDME with 1 wt% KNO_3	76 wt% [≈1.8]	606 [86.96%]	40% [10]	1.2–3.0	42
Solid electrolyte	Sulfur + K_2S_x	K metal [separator-free]	K+-conducting β″-Al_2O_3 solid electrolyte (K-BASE)	Not rep. [not rep.]	402 [98%]	100% [1000]	1.2-3.0	43

3.1 | Cathode

The sulfur cathode is a crucial component of the metal-sulfur battery, which has attracted the most research compared to the anode and the electrolyte.[69,70] Sulfur as cathode endows K-S batteries with high charge-storage capacity (ie, 1672 mA h g^{-1}) and high energy density (ie, 914 Wh kg^{-1}) when coupled with K metal as the anode. The high capacity of sulfur cathode is due to the conversion mechanism where new chemical compounds (eg, K_2S) form by reversible electrochemical reactions, as shown in Equations (1) and (2) in Section 2. The sulfur cathode also brings serious problems, however, including poor conductivity, dissolution of the intermediate products of the electrochemical reaction (ie, polysulfides) into the electrolyte, and large volume changes accompanying the conversion reaction. Its insulating nature makes elemental sulfur unsuitable for direct use as a cathode, so it is often used in combination with additives that have high electronic conductivity (eg, carbon) to improve its electrical contact and sulfur utilization. The polysulfides, intermediate products of sulfur from the electrochemical reaction, can be dissolved into the electrolyte, which may result in loss of active material, capacity fading, and anode corrosion (if polysulfides migrate to the anode, ie, the shuttling effect). The polysulfides should be confined within the cathode during cycling through rational design of the cathode (eg, polysulfide-absorbing substrate), electrolyte (eg, high viscosity electrolyte), and separator (eg, separator with coating). Volume change of the sulfur cathode during the conversion reaction is especially serious for K-S batteries (ie, 309% expansion). The huge volume change induces severe pulverization of the active material during cycling. Substrates with high porosity and a certain amount of flexibility are recommended to accommodate sulfur with such a large volume change. According to the initial form of the sulfur existing in the cathode, the sulfur cathode can be categorized as an S_8 cathode, a small molecular and covalent sulfur cathode, and a polysulfide cathode. The unique advantages and disadvantages of each category will be discussed.

3.1.1 | S_8 cathode

Impregnating sulfur into a conductive porous carbon substrate is the most widely used method to obtain sulfur cathode. The typical method is to heat the mixture of sulfur powder and porous carbon substrate to above the melting point of sulfur (eg, 155°C). Then, molten sulfur impregnates the pores in the carbon substrate driven by capillary forces. The sulfur in S_8 cathode exists in the

form of cyclo-S_8 molecules with molecule size of 0.84 nm within the pores (pore size >1 nm) in the carbon substrate.[71,72] The pore-confined sulfur is usually amorphous, although sometimes crystalline sulfur residues on the carbon surfaces can be observed.[73] The advantage of the S_8 cathode is that it is easy to achieve a large loading capacity (eg, >70 wt% and 10 mg cm^{-2}), which facilitates high energy density. In addition, the large pore size in carbon substrate means that the composite can tolerate the large volume changes that arise from the conversion reaction between sulfur and K ions. Nevertheless, large pores may not provide sufficient absorption and electrical contact to the S_8 molecules inside the pores, leading to low sulfur utilization. In view of this, in most research work, mesoporous carbon with appropriate pore size was used for the substrates.[74-76] Compared to macroporous substrate, the mesoporous substrate provides higher pore volume to achieve high sulfur loading and stronger interactions between sulfur and the porous channels. Since the open pores of the carbon substrate are directly connected to the electrolyte, the active substance S_8 may be pulverized and detached from the substrate due to severe volume changes during potassiation. In addition, the polysulfides are intrinsically polar molecules with the terminal sulfur bearing most of the negative charge.[77,78] The weak interaction between polar polysulfides and the nonpolar carbon substrate is insufficient to anchor the polysulfides, resulting in shedding of polysulfides from the carbon scaffold and migration to the anode (ie, shuttling effect), which causes capacity fade. Therefore, fixing strategies via strong interactions are required to stabilize the cycling. In fact, a variety of fixing strategies, including the introduction of polar heteroatoms (B, N, O, S, and P) and/or functional groups (eg, hydroxyl and amine groups),[79-81] and metal-sulfur bonding (eg, metal-organic frameworks [MOFs], metal sulfides, etc),[82] have been developed to immobilize polysulfides through various interactions such as van der Waals forces, electrostatic adsorption, and Lewis acid/base interactions in Li-S batteries.[83,84] These strategies can be also introduced into the K-S battery to improve its electrochemical performance. In addition, a surface coating strategy is often used in combination with the porous carbon substrate. The external coating layer as a physical barrier can impede the dissolution of polysulfides into the electrolyte, thereby preventing the shuttle effect. For example, due to their high flexibility and conductivity, graphene and conductive polymers such as polypyrrole and polythiophene are used as surface coating substances to alleviate the stress from volume expansion and confine polysulfides.[85,86]

A typical example of an S_8 cathode was reported by Nazar et al for the Li-S battery that used an ordered mesoporous carbon (CMK-3) as the sulfur substrate.[73] The first report of a room temperature K-S battery also adopted sulfur-impregnated CMK-3 as cathode,[36] as shown in Figure 5A,B. The starting cathode was amorphous S_8 in CMK-3, while the discharge product was confirmed to be K_2S_3 by high resolution transmission electron microscope (HRTEM), X-ray diffraction (XRD), and Raman spectra (Figure 5C,D). The gentle slope and a discharge platform (at 1.8 V) observed in the discharge curves indicated two steps of the discharge process. The S_8 was reduced to long-chain polysulfides and then further reduced to short-chain polysulfides, while only a long single platform was detected in the charge process, indicating that the short chain polysulfides were oxidized in one step. At the optimum sulfur content (ie, 40.8 wt%), the CMK-3/sulfur composite displayed an initial discharge capacity of 512.7 mAh g^{-1}, although the capacity quickly decayed to 202.3 mAh g^{-1} (ie, 39.4% capacity retention) after 50 cycles at a current density of 50 mA g^{-1}. The rapid capacity decay was attributed to the shuttle effect, which was indicated by the yellow precipitates on the K anode after 50 cycles. A layer of polyacrylonitrile (PAN) with thickness of 10 nm was further coated on the CMK-3/sulfur composite to improve the capacity retention from 39.4% to 62.9% after 50 cycles, with the CE improving from above 90% to above 95% (Figure 5E). The separator and the K anode were also well protected after 50 cycles by using PAN coated CMK-3/sulfur composite, indicating that the PAN coating was able to impede the solvation of polysulfides. The PAN coating also alleviated the volume expansion stress from potassiation. This pioneering work on the K-S battery proved its feasibility, confirmed the discharge product K_2S_3, and demonstrated the effectiveness of the PAN coating as a physical barrier to inhibit the dissolution of polysulfides. This work also identified other problems for K-S batteries, such as low reversible capacity and rapid capacity decay, so more strategies need to be introduced to develop high-performance K-S batteries.

In addition to surface coating, concentrated electrolyte also inhibits the dissolution and shuttling of polysulfides. The decreased amount of free solvent and increased viscosity of the concentrated electrolyte leads to decreased solubility of polysulfides. Wang et al employed concentrated electrolyte (ie, 5 M potassium trifluoromethanesulfonimide [KTFSI] in diethylene glycol dimethyl ether [DEGDME]) to suppress the dissolution and shuttle effect of K_2S_x intermediates of an S_8 cathode based on CMK-3 porous carbon substrate.[42] This inhibitory function of concentrated electrolyte allowed the K-S battery to operate within a large voltage window of 1.2 to 3.0 V. The custom-made transparent cell setup directly demonstrated the shuttling of polysulfides. In

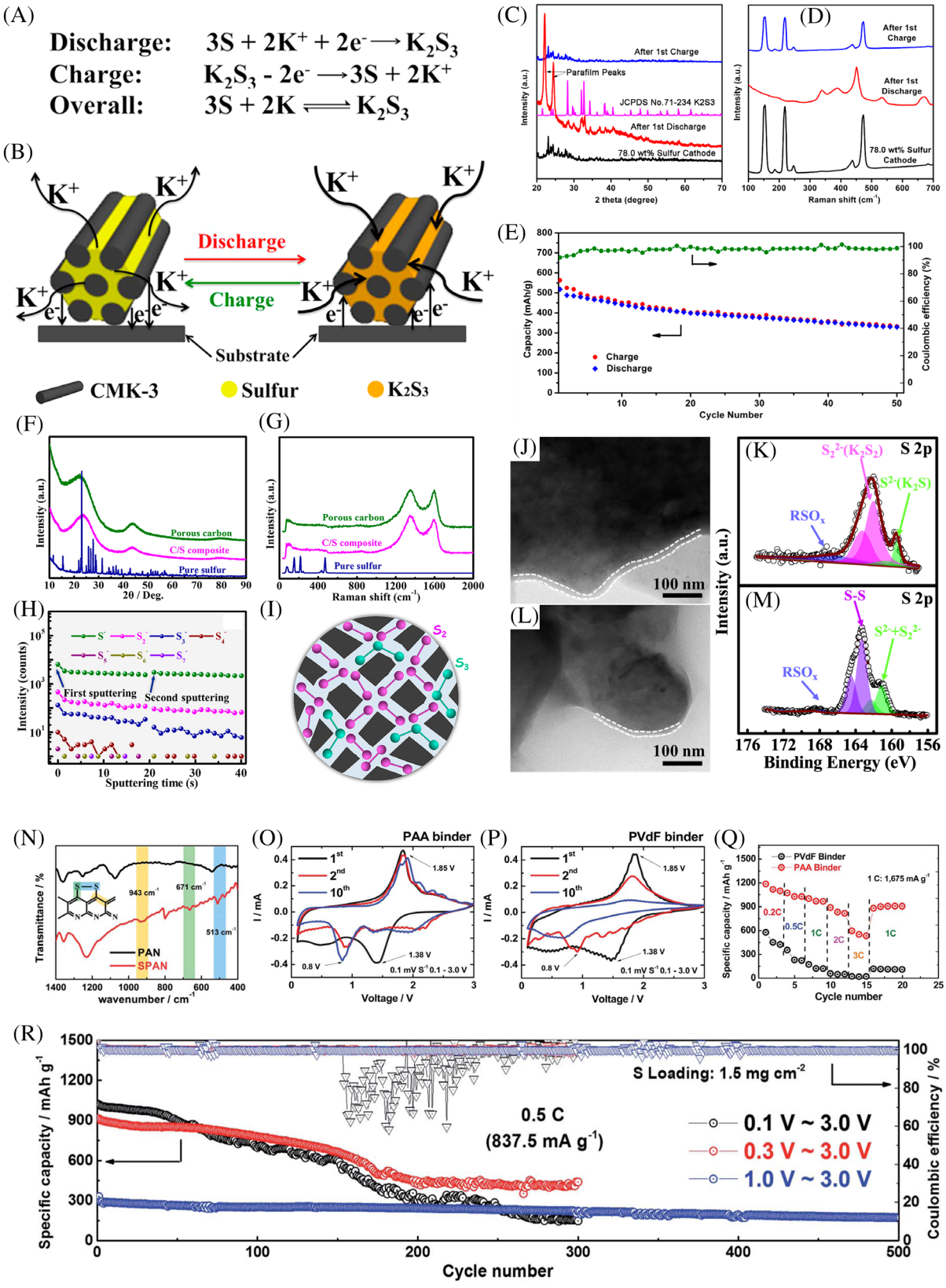

FIGURE 5 Legend on next page.

addition, the electrochemical products formed at different voltages were studied using ex situ XRD by sealing the samples with Kapton tape. The results showed that the reversible stepwise phase transformation was $S_8 \Leftrightarrow K_2S_6 \Leftrightarrow K_2S_5 \Leftrightarrow K_2S_4 \Leftrightarrow K_2S_3$. The final discharge product is K_2S_3, which is consistent with the discharge product reported for the first K-S battery.[36] Unlike Li-S and Na-S batteries,[87] the final discharging product K_2S_3 is formed at a deep discharging voltage of 0.5 V, indicating that the K_2S_3 is the electrochemically stable reduction phase in the K-S battery, which may be due to the low solubility of K_2S_3, K_2S_2, and K_2S.[62] According to the research results by Yiying Wu's group, the insulating, nearly solid-state K_2S and K_2S_2 require the high discharge overpotential of 0.8 V to be formed, even under low current density (ie, 20 mA g^{-1}). The overpotential is so high that the reduction could reach the cut-off potential before the formation of K_2S_2 phase. These results indicate the difficulty for the K-S battery, compared to Li-S and Na-S, in terms of fully utilizing the capacity of sulfur (ie, to obtain K_2S phase). Further research work is still needed to improve the sluggish reduction kinetics of the K-S battery associated with insulating, solid-phase products such as K_2S_3, K_2S_2, and K_2S. Besides CMK-3, a binder-free carbon nanofiber (CNF) paper has been adopted as substrate for the S_8 cathode of the K-S battery.[40] A thin layer of single-wall carbon nanotube (SWCNT) coated separator was also used in combination with the CNF/sulfur cathode to sandwich the sulfur active material between the CNF matrix and the SWCNT coating. This unique sandwich structure ensures good electrical contact of the polysulfides intermediates, thus improving sulfur utilization. Therefore, a high discharge capacity of 1144 mA h g^{-1} was achieved. Moreover, no sulfur element was detected on the K anode after cycling, which indicated that the SWCNT coating effectively confined the polysulfides within the cathode side. The discharge product at different voltages was studied by various characterization methods, including ultraviolet-visible (UV-Vis) spectroscopy, XRD, X-ray photoelectron spectroscopy (XPS), and Raman spectroscopy. The transition processes of elemental sulfur (existing as S_8) can be briefly illustrated as $S_8 \leftrightarrow K_2S_6 \leftrightarrow K_2S_4 \leftrightarrow K_2S_2 \leftrightarrow K_2S$ in the voltage window of 1.0 to 2.8 V. Although a K-S battery with high discharge capacity was successfully demonstrated using the sandwich structure, the cyclability was limited (ie, 50 cycles), and the capacity decayed quickly, which may be due to the pulverization and loss of sulfur active material during cycling.

3.1.2 | Small molecular and covalent sulfur cathode

When the pore size of a microporous substrate is less than 0.7 nm, the sulfur can only exist within the pores in the form of small molecular sulfur (ie, S_n, $n \leq 4$).[54,6088,89] The electrochemical reaction process of small molecular sulfur is different from that of the S_8 cathode. During discharging, small molecular sulfur (eg, S_4) is transformed to low-solubility short chain polysulfides or K_2S through a solid to solid transition. During charging, the solid state short chain polysulfides or K_2S are changed back to S_n ($n \leq 4$) rather than S_8 due to the space confinement of small micropores. As no soluble long chain polysulfides are formed during the charge-discharge process, the dissolution and shuttle effect of polysulfides can be avoided for small molecular sulfur cathode. Furthermore, microporous substrates with small pores provide better conductive contact and stronger interaction with sulfur inside the pores, allowing high sulfur utilization. Unlike S_8 cathode, however, small molecular cathode usually has low loading (eg, < 1 mg cm^{-1}). Xiong et al reported the room-temperature K-S batteries fabricated using small-

FIGURE 5 A, Electrochemical reactions for discharge, charge, and overall processes of the K-S battery. B, Schematic diagram of the electrode reactions of rechargeable K-S batteries. C, X-ray diffraction (XRD) patterns with selected states after the first charge and the first discharge in comparison with the standard JCPDS card of K_2S_3. D, Raman spectra for selected processes after the first charge and the first discharge in comparison with the pristine cathode. E, Cycling performance and Coulombic efficiency at a current rate of 50 mA g^{-1}. A-E, Reproduced with permission. Copyright 2014, American Chemical Society.[36] F, XRD patterns of pure sulfur, porous carbon, and the microporous C/S composite. G, Raman spectra of pure sulfur, porous carbon, and the microporous C/S composite. H, The time-of-flight secondary ion mass spectrometry (TOF-SIMS) data of the microporous C/S composite. I, Schematic illustration of the existing forms of sulfur in the porous carbon matrix: S_2 (purple) and S_3 (green). J, Transmission electron microscope (TEM) image and K, the high-resolution S 2p X-ray photoelectron spectroscopy (XPS) spectrum of the microporous C/S composite electrode in the fully discharged state. L, TEM image and (M) the high-resolution S 2p XPS spectrum of the microporous C/S composite electrode in the fully charged state. F-M, Reproduced with permission. Copyright 2019, American Chemical Society.[60] N, Fourier transform infrared spectroscopy (FTIR) analysis of polyacrylonitrile (PAN) and sulfurized PAN (SPAN). O, Cyclic voltammograms of the SPAN electrode with the PAA binder. P, Cyclic voltammograms of the SPAN electrode with the polyvinylidene difluoride (PVDF) binder. Q, Rate capability test (sulfur loading amount in the SPAN electrode: 0.8 mg cm^{-2}). R, Long-term cycling performance with a relatively high sulfur loading of 1.5 mg cm^{-2} in the SPAN electrode. N-R, Reproduced with permission. Copyright 2018, Royal Society of Chemistry[39]

molecule sulfur stabilized by sucrose-derived microporous carbon as cathode (Figure 5I).[60] The existing form of sulfur in the microporous carbon (pore size <1 nm) was confirmed to be mostly S_2 and S_3 by time-of-flight secondary ion mass spectrometry (TOF-SIMS, Figure 5H). Trace amounts (ie, 0.14%) of S_4 to S_7 molecules might have arisen from residual sulfur molecules on the surface. The authors demonstrated that the fragmented sulfur (ie, S_2 and S_3) was absorbed strongly by carbon atoms within the micropores by showing the high stability of the small molecule sulfur composite in different experiments. For example, the composite showed high sulfur retention (20 wt%) under 300 keV electron beam irradiation compared to bulk cyclo-S_8 (2 wt%). In addition, the decomposition temperature of the composite was 400 to 600°C, which is much higher than the evaporation temperature of the pristine cyclo-S_8 (~300°C). The depotassiation reaction voltages (ie, 1.65 and 1.95 V) of small molecule sulfur composite were lower than those for cyclo-S_8 electrodes (ie, ~1.8 and ~2.4 V), showing different reaction mechanisms due to the different sulfur structures. The absence of soluble long chain polysulfides in the electrochemical reactions results in the disappearance of the high voltage platform in the charge-discharge curves of small molecular sulfur cathode. When using this small molecular sulfur cathode, the K-S battery showed a reversible capacity of 1198.3 mA h g^{-1} and 72.5% capacity retention after 150 cycles with a CE of ~97%. XPS in the discharge state showed the signals of RSO_x species (assigned to the SEI), S_2^{2-} (assigned to K_2S_2), and S^{2-} (assigned to K_2S), indicating that K_2S was the discharging product (Figure 5K,M). In the charge state, most sulfide species were oxidized to S-S, although residual sulfide species were still detected, indicating that the oxidation reaction was incomplete. Although the polysulfide shuttle was avoided, the XPS results showed that there was still capacity loss at each cycle. The possible reasons could be the sluggish kinetics, high SEI impedance, and large volume changes of the K-S battery.

Both S_8 and small molecular sulfur (ie, S_n, $n \leq 4$) are confined within the conductive matrix by interfacial immobilization between sulfur and the surface of the matrix via physical confinement and chemical adsorption. In contrast, covalent sulfur cathode incorporates sulfur via covalent bonds, which enables high dispersibility and utilization, and strong immobilization of the active sulfur. The strong covalent bonds between sulfur and the conductive substrate also inhibit the migration of polysulfides, thereby suppressing active sulfur loss and the shuttle effect. The covalent sulfur cathode is fabricated from sulfur-embedded polymers, which are obtained by incorporating sulfur chains into polymers. The sulfur-embedded polymers can be categorized as sulfurized polymers and sulfur copolymers. Sulfurized polymer contains short chain sulfur within the carbon polymer chain and has low sulfur content, while sulfur copolymer has long polymeric sulfur chains and high sulfur content. As a typical example, sulfurized polyacrylonitrile (SPAN) prepared by the reaction between sulfur and PAN at high temperature in a protective atmosphere has been widely studied.[85] In this reaction, PAN is first dehydrogenated to form a conjugated cycle-like structure, and then the cycle-like aromatic structure is sulfurized by sulfur fragments to form SPAN. The reaction temperature determines the sulfur distribution and content in the SPAN. The covalent sulfur content was 30 to 55 wt% in the synthesis temperature range of 280°C to 550°C. The covalent sulfur exists in short chains with the chain length no greater than S_4. Therefore, the soluble long chain potassium polysulfides are intrinsically avoided in the SPAN cathode. The reaction mechanism of SPAN with Li ions has been extensively investigated in Li-S batteries.[90] In the discharge process, the pristine SPAN first makes a transition to radical SPAN through cleavage of C-S bonds. Then, the radical SPAN is lithiated to form ionic SPAN through two pathways: (1) lithium ions are hosted at the negative sites around both sulfur and pyridine N atoms; and (2) lithium ions are hosted only at the negative sites around sulfur. In the charge process, the ionic SPAN is converted back to radical SPAN rather than pristine SPAN. To date, the SPAN cathode is the most widely used cathode for K-S batteries, as shown in Table 3.[38,41,66,67]

Liu et al fabricated a room temperature K-S battery using SPAN with sulfur content of 38 wt% as the cathode. The K-S battery showed a high reversible capacity of 710 mA h g^{-1} and good rate performance.[38] The cycling stability was poor, however, and the capacity decayed quickly. The authors observed that the separator became yellowish after 500 cycles, and the impedance of the K-SPAN cell increased with cycling from the first to the 50th cycle. These observations implied that the capacity fading may be associated with the nonelectrochemical decomposition of the electrolyte, which leads to reaction polarization during cycling. Therefore, both optimization of the electrolyte composition and SPAN cathode design are needed to reduce the polarization and improve the cyclability. To improve the conductivity of SPAN, iodine-doped sulfurized polyacrylonitrile (I-S@PAN) was reported by Ma et al to be used as Na-S and K-S cathodes.[66] Raman spectra showed that there was no elemental sulfur or elemental iodine, indicating that both iodine and sulfur were doped into the PAN, existing in the form of covalently bonded chains. As K-S battery cathode, the I-S@PAN presented a high initial capacity of 1448 mAh g^{-1} at 0.1 C and a reversible capacity of

722 mAh g^{-1} after 100 cycles. Due to the iodine doping, however, the sulfur content in I-S@PAN was reduced to 17.7 wt%, which affected the energy density of the K-S battery. Hwang et al reported a room temperature K-S battery with high reversible capacity (ie, 1050 mAh g^{-1}) and cycling stability (95% retention after 100 cycles) that used a SPAN cathode coupled with PAA binder.[39] FTIR showed the existence of C-C bonding (yellow), C-S bonding (green), and S-S bonding (blue) of SPAN cathode (Figure 5N). Cyclic voltammograms showed the high reversibility of SPAN cathode with PAA binder, while the SPAN cathode with polyvinylidene difluoride (PVDF) binder experienced a significant decrease in its oxidation-reduction peak intensity after the first cycle, indicating an irreversible redox reaction (Figure 5O,P). The SPAN/PVDF cathode exhibited inferior performance with an initial discharge capacity of 370 mAh g^{-1} and a capacity retention of 22% after 100 cycles. This is because the PAA-based binder provided better adhesion to the SPAN electrodes compared to the PVDF binder, thus achieving high uniformity and structural stability of the SPAN cathode during large volume changes by potassiation. The lower impedance of SPAN/PAA cathode compared to SPAN/PVDF cathode indicated that the PAA binder facilitated the formation of a stable SEI with lower charge transfer resistance. The discharge product at the deep discharge voltage of 0.1 V was determined to consist of K_2S and K_2S_2 compounds by XPS. The authors also studied the long-term cycling performance of the SPAN/PAA cathode upon the different discharge COVs (Figure 5R). At a high COV, the cathode showed excellent cyclability with capacity retention of 70% at 500 cycles at 0.5 C. At a low COV, the initial capacity was much higher, although it decayed quickly after 300 cycles, which was attributed to the large volume expansion from the C-S bonds to the final product K_2S. As the most commonly used K-S cathode, SPAN often gives high reversible capacity (ie, 638-1050 mAh g^{-1}) and a relatively long cycle life (ie, 100-500 cycles), however, although this high performance is, to some extent, based on the low sulfur content of SPAN cathode (<45 wt%). To improve its practicality, the research on SPAN cathode should focus on improving its sulfur content.

3.1.3 | Polysulfide cathode

Dissolved polysulfide in an organic electrolyte has been employed as cathode in two types of Li-S batteries, the Li-polysulfide redox flow battery and the Li-polysulfide battery.[91,92] In contrast to the solid-state insulating property of S_8 or Li_2S as the starting active material in the cathode, the liquid active polysulfide material possesses better initial redox kinetics, a more homogeneous distribution in the conductive substrate, and improved charge transfer at the interfaces between the polysulfide and the conductive substrate.[91,93,94] Furthermore, a free-standing, binder-free cathode, without a current collector and with high areal loading and utilization of active material, is readily fabricated using liquid polysulfide and a conductive substrate, which facilitates high energy density of the whole cell. Like other active sulfur materials (eg, S_8 and Li_2S), polysulfide cathode can also experience the full range of sulfur redox reactions (ie, S_8 to polysulfides to Li_2S). Therefore, polysulfides as starting materials can be either reduced to Li_2S or oxidized to S_8 in the electrochemical reactions. The Li_2S or S_8 converted from the uniformly distributed polysulfide also has a very uniform distribution and good conductive contact with the substrate, which facilitates good kinetics for subsequent electrochemical reactions. Recently, the polysulfide cathode has also been adopted for the K-S battery. Hwang et al reported a room temperature K-S battery using K_2S_n ($5 \leq n \leq 6$) catholyte absorbed in a 3D free-standing carbon-nanotube film (3D-FCN-film) as cathode.[39] The polysulfide cathode in this K-S battery was bifunctional, providing active sources and acting as a K^+-conducting medium. The K-S battery presented a high discharge capacity of ~400 mAh g^{-1} at the 0.1 C-rate with excellent cycling stability (94% retention after 20 cycles) and good rate capability up to the 2 C-rate. The discharge product was confirmed to be K_2S_3 by ex situ XRD, so a reversible conversion reaction occurred between K_2S_n ($5 \leq n \leq 6$) and K_2S_3. The authors also demonstrated the feasibility of a high-safety K-S full battery using K_2S_n ($5 \leq n \leq 6$) as cathode and K ion impregnated hard carbon as anode. This full battery delivered a high initial discharge capacity of 235 mAh g^{-1} at the 0.1 C-rate (1 C rate: 558 mA g^{-1}) in the voltage range of 0.7 to 1.85 V, which provides a new opportunity for high-safety K-S batteries. Although polysulfide as K-S cathode is still in its infancy, it is likely to represent the future research direction because of its unique advantages with practical cell parameters (ie, high sulfur content, lean electrolyte, etc), as it can avoid the need for the current collector and binder, which facilitates the use of lean electrolyte. Therefore, more attention should be paid to the polysulfide cathode.

3.2 | Anodes

3.2.1 | Basic understanding of potassium metal

As the anode, K metal has a low redox voltage (K^+/K: −2.93 V vs SHE) and high specific capacity (687 mAh g^{-1}) in comparison to other types of anodes (eg, carbonaceous,

alloying, and intercalation compounds),[95-100] thus endowing K-S batteries with high operating voltage and energy density. Nevertheless, the practical use of K metal as anode remains a big challenge due to many technological and safety concerns.[97,101] As with Li metal anode, an SEI spontaneously forms on the interface between the K metal and organic electrolyte compounds.[102] This SEI formation is inevitable, due to the fact that the Fermi energy of K metal is higher than the lowest unoccupied molecular orbital (LUMO) of ester and ether solvents, which are the two most widely used solvents for liquid electrolyte. In order to maintain a high CE and long lifespan, the SEI on the K metal surface should be chemically stable, metal ion-conductive, uniform and compact with a well-defined structure coupled with mechanical rigidity and elasticity to accommodate the volume changes and to avoid localized effects promoting dendrite growth.[103,104] Stable K plating and stripping is pivotal in obtaining such an ideal SEI. Unfortunately, obtaining uniform and stable K plating and stripping during cycling is quite challenging. In fact, metal anodes are plagued with unstable plating and stripping, which results in an unstable SEI with high roughness and an inhomogeneous surface. Such an unstable SEI surface is easily fractured to expose the fresh K metal under the SEI surface, which subsequently reacts with the electrolyte to form new SEI. In addition, long dendrites may grow and break from the SEI surface, forming isolated electrochemically inactive "dead" K.[41] This continuous cracking/re-construction of SEI as well as "dead" K during cycling cause consumption of both the active anode material and the electrolyte, with a severe increase in impedance, leading to low CE, poor reversibility, and short lifespan. Even more severe are the potential safety hazards (eg, combustion and explosion) caused by an internal short circuit when the resulting K dendrites penetrate the separator and reach the cathode.[39,41] In the case of K-S, the dendrites or fractured SEI on K metal anode can even react with polysulfides (shuttling from the cathode) to induce corrosion of the K metal anode, leading to many severe issues (eg, active sulfur loss, self-discharge, capacity fading during cycling, etc).[105] This K anode corrosion by polysulfides can be observed from the precipitation of some insoluble sulfides on the surface of the K anode or on the side of the separator near the anode.[62]

The current state-of-the-art K-S batteries are mostly assembled using oversized or excessive amounts of K metal. Cycling with this excess amount of K metal anode induces less volume change for the anode and makes all the above problems less negative, because only a small fraction of the K metal anode is involved in the cycling. For example, plating and stripping the top 10 μm of a 200 μm K foil leads to only a 5% change in electrode height.[17] This optimistic scenario arising from the excess amount of K metal may result in misconceptions on the electrochemistry of the K-S battery and underestimation of the hazards regarding K dendrites or inhomogeneous K deposition. In a practical K-S battery, the excessive K metal anode jeopardizes the cell's gravimetric capacity and gravimetric energy density. Therefore, an ideal K-S full cell would operate at the areal capacity ratio of the positive to the negative electrode of 1.[106] Although a little excess amount of K anode is required to offset the anode loss owing to the reaction between K and the electrolyte to form the SEI,[106] nearly the entire K metal anode would be stripped and deposited during each discharge-charge cycle, associated with huge volume changes at every cycle.[17] In these circumstances, the internal stress within the K metal caused by such a large volume change is likely to induce more severe cracking and reforming of the SEI, making problems such as low CE and short lifespan more pronounced. Therefore, thin K metal anodes that are well matched to the sulfur cathode (areal capacity ratio between them approaching to 1) should be used in future K-S research to obtain a better understanding of the K-S electrochemistry under practical conditions and to accelerate its practical applications.

The SEI on the K surface consists of complex composite including a K-containing salt (eg, KF, K_2O, K_2CO_3, $ROCO_2K$, etc) and reduction products (eg, formate and acetate) of the electrolyte. The composition of the SEI varies depending on the specific electrolyte salt and solvent used. The multiple internal interphase interfaces among the heterogeneous salts and grains in the SEI provide solid-state paths for fast K ion diffusion. Thus, the SEI both passivates the K surface and conducts K ions to enable reversible electrochemical processes for K deposition and dissolution.[99] Many researchers have pointed out that the SEI is intrinsically heterogeneous in terms of structure, composition, mechanical properties, ion diffusion rate, and so forth.[99,100,107] For example, the composition of the SEI is heterogeneous, with organic salts on the outside and inorganic salts on the inside.[107] The quality of the SEI (ie, stability, ion diffusion rate, impedance, etc) that determines the K metal anode performance is strongly affected by the electrolyte formula. Analysis of this impact provides a better understanding of the electrochemistry of the K plating and stripping and the interaction between the electrolyte and the K anode (eg, passivation, etc). For example, one electrolyte formula (ie, potassium bis(fluorosulfonyl)imide [KFSI] salt in dimethoxyethane [DME]) enables reversible K plating and stripping over the long term while other electrolyte formulas such as 1 M KPF_6-DME, 1 M KTFSI-DME, and 0.8 M KPF_6-EC/DEC all failed to perform reversible K plating/stripping due to rapid capacity decay.[99] It was also reported that the polarization of K metal was

decreased by increasing the concentration of electrolyte salt. The reduced polarization can be attributed to the lower resistance and greater durability of the SEI formed in the highly concentrated electrolyte.[108] Nevertheless, the polarization of K metals still is larger than those of Li and Na metals, even when a highly concentrated electrolyte (ie, 3.9 M potassium bis(fluorosulfonyl)amide (KFSA)/DME) is used. Besides the electrolyte salt and solvent, the additive is also an important electrolyte component that is used to enhance the stability of the SEI. Although additives such as fluoroethylene carbonate (FEC), difluoroethylene carbonate (DFEC), and vinylene carbonate (VC) have worked efficiently in K ion batteries, they have no positive effect on K metal plating.[108] These results imply that K metal anode may need a special additive that differs from those used for K ion batteries, and further development of efficient electrolytes and additives is urged to enhance the electrochemical performance of K metal batteries.

3.2.2 | Strategies toward dendrite-free K anode

K dendrites cause severe issues such as active K anode loss, electrolyte depletion, severe impedance rise, self-discharge, capacity fading during cycling, and so forth, thus, preventing the utilization of K metal anode. Developing a dendrite-free K metal anode is critical to avoid all these issues, and many efforts have been devoted to this aim. Although research to prevent K dendrites is still in its infancy, there have been many techniques that have been proved successful for stabilizing Li metal anode (ie, preventing Li dendrite formation or proliferation in Li-metal batteries). Many of these techniques could be grafted onto stabilizing K metal anode. To date, several strategies have been proposed to obtain dendrite-free or dendrite-suppressed K metal anodes with long-term reversible cycling, including concentrated electrolyte,[42,99,108] self-healing,[109] artificial SEI on K metal anode,[110] a functional anode substrate (eg, MXene as substrate),[41,111] and K-Na alloy.[100]

Concentrated electrolyte

Concentrated electrolyte offers technical superiority in terms of figure of merit over alternative materials. By simply increasing the salt concentration in a suitable solvent to above a threshold (usually >∼3-5 M depending on the salt-solvent combination), the free solvent molecules disappear, and the location of the LUMO shifts from the solvent toward the salt, resulting in the reductive decomposition of the salt before the solvent at low potential.[112,113] This unique property produces a salt-derived SEI in concentrated electrolyte rather than a solvent-derived SEI as in a normal electrolyte. The salt derived SEI has high stability and a high transport number, giving the battery several advantages, such as a long cycling life and a wide operating temperature range. The concentrated electrolyte also has a high level of safety (ie, fire-extinguishing, nonvolatile) and is capable of high voltage operation because there is no free solvent.[112] Recently, concentrated electrolyte has also been demonstrated to be effective for K metal anode.[42,99,108] For example, Xiao et al reported dendrite-free potassium plating and stripping with excellent electrochemical stability up to 5 V (vs K/K^+) using superconcentrated KFSI in DME electrolyte.[99] Because there are fewer free solvent molecules in concentrated electrolyte that can be reduced by the K metal, the initial CE is higher than that of batteries using normal electrolyte. The long-term reversibility of the K metal anode was due to the compact SEI, which impedes side reactions and keeps the K electrode dendrite-free during cycling. Hosaka et al demonstrated that the concentrated electrolyte was capable of suppressing polarization during cycles of K plating-stripping, resulting in the smallest overpotential of ∼50 mV when using a highly concentrated electrolyte consisting of 3.9 M $KN(SO_2F)_2$/1,2-dimethoxyethane (Figure 6A).[108] The K anode stability under different electrolytes were also investigated. For low concentration electrolytes (ie, <1 M), both the plating/striping curves and immersion experiment (ie, discoloration of K metal immersed in the electrolyte after 14 days) showed that the EC:DEC was superior to PC for both KPF_6 and KFSA salts (Figure 6A). Furthermore, the electrochemical performance of KFSA was better than that of KPF_6 in EC:DEC. The effects of additives on the electrolyte performance were also studied based on the KPF_6 in EC:DEC electrolyte and the results showed that the additive-free electrolyte was better than the ones with additives (ie, FEC, DFEC, or VC). Therefore, the KFSA in EC:DEC was the best electrolyte in low concentration electrolytes. When it was compared to concentrated electrolyte, however, its performance was inferior to that of 3.9 M KFSA in DME electrolyte. The enhanced electrochemical performance of concentrated electrolyte with low polarization is due to the lower resistance and higher durability of the SEI formed in the concentrated electrolyte. Recently, Wang et al applied concentrated electrolyte in K-S batteries and achieved a high discharging voltage of 2.1 V, delivering a discharging energy density of ∼1270 Wh kg^{-1}.[42] The high electrochemical performance of K-S batteries was ascribed to the impeded dissolution and shuttle reactions of K_2S_x intermediates in the concentrated electrolyte, even at a high charging voltage of 3.0 V. Although some superior electrochemical performance was achieved

using concentrated electrolyte, the capacity faded quickly, and the cycling stability was poor in these K-S batteries with concentrated electrolyte.

Self-healing

Metal dendrites are kinetically highly favorable during extended cycling. The nucleation and growth of dendrites are even accelerated on a thick, nonuniform, and heterogeneous SEI, owing to the uneven migration of K ions through such SEI layers. Hundekar et al proposed a strategy to obtain self-healing of K dendrites by controlling the current density.[109] The mechanism behind self-healing is the internal self-heating within the battery under high current density, which triggers extensive surface migration of K atoms away from the dendrite tips, thereby smoothing the dendritic surface. The self-heating phenomenon is known as a negative attribute, as it can cause thermal runaway, and in a severe case, a catastrophic fire hazard. Hundekar et al showed that even this negative attribute, if controlled properly, can be used to smooth dendrites.[114,115] More surprisingly, they discovered that the self-healing process in K anode is more efficient than that in Li metal. The underlying reason for this behavior was revealed by detailed DFT calculations, which is ascribed to the greater mobility and lower energy barriers of surface K atoms relative to Li metal atoms (Figure 6B-F), thus enabling self-healing of K dendrites to take place at an order-of-magnitude lower current density.[109] The SEI formed under a healing current density of 2 mA cm^{-2} was observed to be more uniform and thinner than that of the SEI obtained at low current densities. The dendrites probably re-nucleate due to the enhanced uniformity and reduced thickness of the SEI layer under the healing current density.

Artificial solid-electrolyte interphase

The artificial solid-electrolyte interphase (ASEI) strategy has been demonstrated great potential for preventing dendrites on Li and Na metal anodes. For example, carbonaceous coatings (eg, carbon nanotubes [CNTs],[116] graphene,[117] and graphite[118]) on Li and Na metal anodes have been proven to be efficient ASEI layers. This strategy has recently been adopted to address the physicochemical instabilities of the K metal surface. Wang et al demonstrated long-term SEI stabilization, high-capacity deposition, and dendrite-free K cycling by simply coating a layer of CNT film on the surface of a K metal anode.[110] Because of its dendrite-free feature, the CNT-coated K metal anode achieved an unprecedented cycle life (over 1000 cycles, over 2000 hours) at a high current density of 5 mA cm^{-2} and an attractive areal capacity of 4 mAh cm^{-2}. The CNT film was coated on the K metal foil by a simple contact method between both parts in electrolyte solution. By doing so, the spontaneous reduction of electrolyte and potassiation of CNTs took place, forming a stable SEI layer on the surface of the potassiated CNT film, as evidenced by ex situ TEM observations (Figure 6G-L) and XPS characterization (Figure 6M) on the SEI layers formed on the surface of the CNTs. This induces a "potassiophobic-potassiophilic" transition in the CNT framework. Another advantage of potassiated CNTs is their high chemical affinity with metallic K, making it possible to regulate and guide K nucleation within the entire CNT film. As a result, the potassiophilic CNT coating acts as an ideal host for the K anode to confine the stripping/plating of K within the CNT framework, thus eliminating the nonhomogeneous electrodeposition of potassium.[110]

K anode host design

Confining K metal in a 3D conductive matrix to form a mixed conducting network is believed to suppress the growth of K dendrites by accommodating the volumetric changes of K anode during plating/stripping cycles, while simultaneously reducing the local current density by spreading the ion flow laterally.[41,119] This strategy has been successfully used to stabilize metallic Li and Na anodes.[120,121] Typically, the construction of such an alkali metal/conductive matrix network is achieved by a melt infusion or electrodeposition method, which sometimes needs additional pretreatments such as heteroatom doping,[122,123] coating,[121,124] or the introduction of functional groups[120] on the conductive framework to improve the wettability of the conductive matrix for molten alkali metals. Recently, a similar melt infusion method without any pretreatments was used to encapsulate K metal in a conductive aligned CNT membrane (ACM).[111] This aligned structure produces strong capillary forces to improve its wettability toward molten K and provides a large pore volume to store K metal. The as-prepared K-ACM anode shows stable plating/stripping profiles with low polarization compared with bare K electrode at various current densities (Figure 6N-Q). More remarkably, excellent cycling stability and rate capability were achieved when a K-ACM anode was paired with a Prussian blue cathode in a full cell, confirming the excellent suitability of K-ACM anode.[111] In addition to carbonaceous conductive matrices, MXene, a 2D material with high conductivity, has also been used as the host for K metal to obtain dendrite-free K anode. Very recently, Tang et al reported titanium-deficient nitrogen-containing MXene/CNT free-standing scaffold (DN-MXene/CNT) as a K metal host to control nucleation behavior and suppress dendritic growth.[41] The K@DN-MXene/CNT anode was obtained by the melt infusion method, taking advantage of the low melting point of K (~63°C).

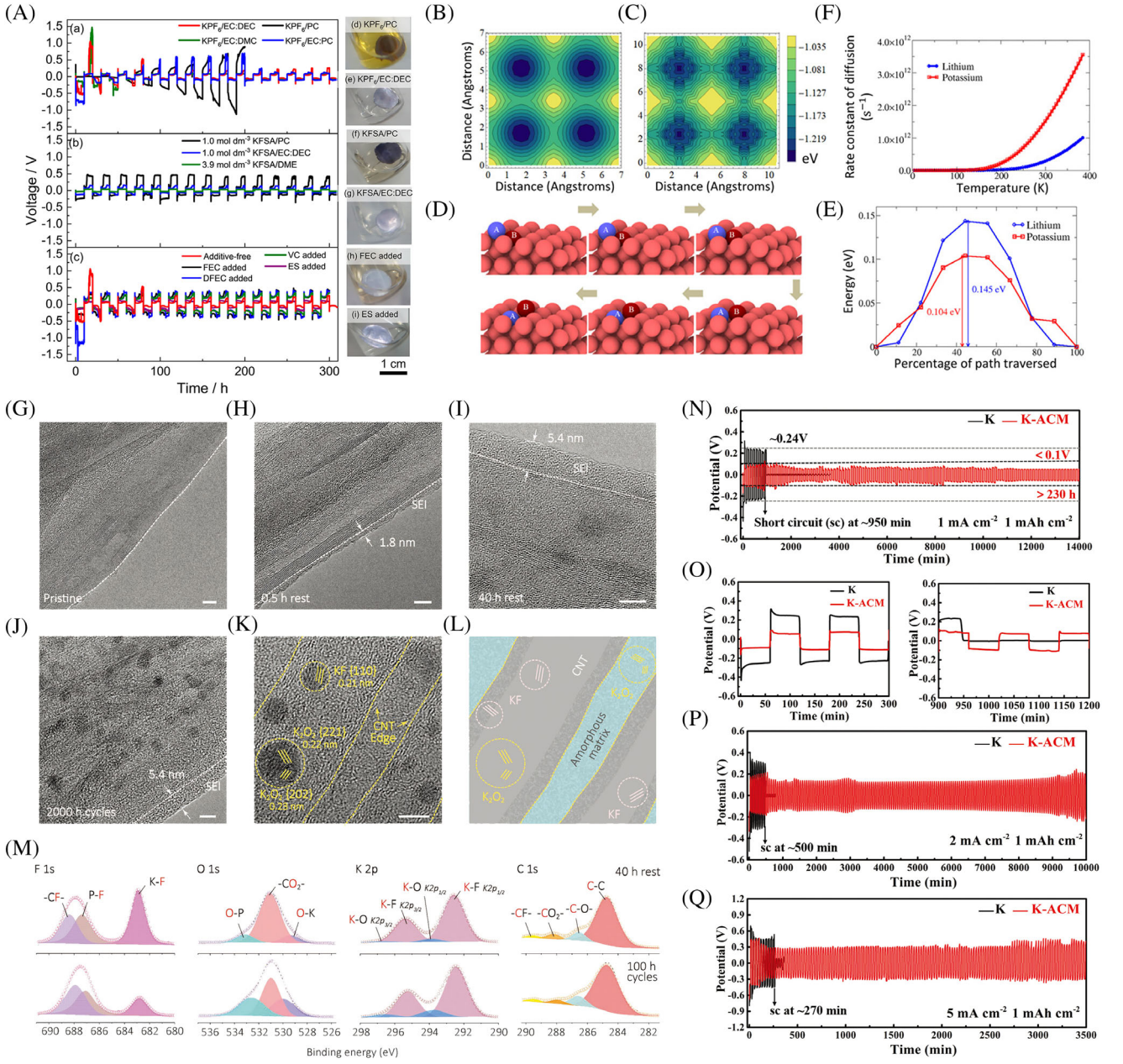

FIGURE 6 A, Voltage profiles of repeated K plating-stripping in various electrolytes with different solvents, and different concentrations and additives in K//K symmetrical cells with photographs of K metal discs in different electrolytes after 14 days. Reproduced with permission. Copyright 2019, American Chemical Society.[108] B-F, First-principles DFT calculations on the surface diffusion characteristics of Li and K metal: Adsorption energy landscape for (B) Li adatom on Li (001) and (C) K adatom on K (001); D, Snapshots of the atomic configuration along the minimum energy path (MEP) for self-diffusion, with the adatom in a 4-fold hollow in the exchange mechanism; E, The calculated activation energy barrier via the MEP method for the diffusion by exchange mechanism for Li and K; F, The calculated variation of the diffusion rate constant with temperature for both Li and K. Reproduced with permission. Copyright 2020, National Academy of Sciences.[109] G-M, Morphology and XPS spectra of SEI layers formed on the surfaces of CNTs: TEM images of (G) pristine CNT, and CNT lifted from the surface of the K foil after resting in 0.5 m KPF_6 EC/DEC electrolyte for (H) 0.5 hour and (I) 40 hours, and (J) after 2000 hours of cycling in a coin-type K/CNT|K/CNT symmetric cell. K, TEM image and L, the corresponding schematic illustration of the observed mosaic structure of the SEI. Scale bar, 5 nm in (G)-(K). M, XPS spectra of the SEI layers formed on the surfaces of CNTs after 40 hours rest (upper) and 100 hours of cycling (bottom). Reproduced with permission. Copyright 2019, Wiley-VCH.[110] N-Q, Electrochemical performance of symmetric cells with bare K or K-aligned carbon nanotube membrane (K-ACM) electrodes: Galvanostatic cycling tests at different current densities of (N) 1 mA cm^{-2}, (P) 2 mA cm^{-2}, and (Q) 5 mA cm^{-2} with a stripping-plating time of 2 hours and capacity fixed at 1 mAh cm^{-2}; and (O) selected specific voltage profiles at 1 mA cm^{-2}. Reproduced with permission. Copyright 2019, Wiley-VCH[111]

The molten K could be directly absorbed into the as prepared MXene scaffold due to its potassiophilic property. This porous scaffold with abundant interconnected voids enabled massive loading of metallic K and preserved a constant electrode dimension during cycles of plating/stripping. K@DN-MXene/CNT showed a dendrite-free morphology with high CE and long cycle life during plating/stripping processes. When tested in K-S full batteries, such anodes also delivered enhanced specific capacity and cycling performance compared with bare potassium metal anodes.[41] The mechanisms by which these conductive matrices (ie, ACM, DN-MXene/CNT, etc) suppress dendrites are similar: (a) They have porous and robust skeletons to load metallic K and to mitigate dimensional changes of the whole electrode during cycling. (b) They are K-philic, which is very important for them to act as "seed points" to initiate the K nucleation during cycling, thereby preventing the direct plating of K outside of the scaffold. (c) They have high electronic conductivity to reduce the effective local current density and to facilitate a uniform K ion flux. These features set the standards for designing dendrite-free K-anode matrices.

3.2.3 | K-based anodes beyond K metal anodes

Besides the K metal anode, many other types of K-based anodes (eg, K-Na alloy, potassium biphenyl complex [BpK], K impregnated hard carbon, etc) have been proposed to circumvent the dendrite issues in K metal anodes. These K-based anodes are intrinsically dendrite-free anodes, thus allowing for a stable SEI layer. These K-based anodes have demonstrated superior electrochemical performance in K ion batteries[100] or K-O_2 batteries,[125] which implies that they are potential alternative anodes for K-S batteries. In this regard, more future research is encouraged to design K-S batteries based on these K-based anodes.

Goodenough and co-workers first proposed liquid K-Na alloy, a room temperature eutectic, as anode for potassium ion batteries.[100] Its biggest advantage is that it does not grow dendrites due to the surface tension forces of the liquid K-Na alloy. At 25°C, the dendrite-free liquid extends from 9.2 to 58.2 wt% Na. This liquid zone could deliver a high specific capacity of 629 mA h g^{-1} for a Na-metal battery and 579 mA h g^{-1} for a K-metal battery. As liquid K-Na alloy is immiscible with most hydrocarbons, it can form a liquid electrode in liquid electrolyte, which changes volume during charge/discharge cycling. This unique feature allows the K-Na alloy anode to be used in liquid electrolyte. Typically, K-Na alloy is absorbed in a porous substrate to be fabricated into a sheet electrode. The absorption process is not spontaneous, however, because the K-Na alloy does not wet the carbon matrix at room temperature due to strong surface tension of K-Na liquid (ie, stronger bonding with itself than with most surfaces). To solve this problem, several methods have been developed to enhance the wettability of liquid K-Na alloy, including increasing the temperature to 420°C and room temperature infiltration based on oxidation of the alloy or vacuum infiltration.[100,126,127] To date, the liquid K-Na alloy anodes have been applied in K ion and K-O_2 batteries.[100,125] Due to their dendrite-free feature, the liquid K-Na alloy anode exhibits stable and long-term plating and stripping processes (eg, for 2800 hours) with an acceptable overpotential of 0.4 V.[32]

Liquan Chen et al reported another class of liquid anodes fabricated by dissolving alkali metal into a mixed organic solution of biphenyl and ethers.[128] As a proof-of-concept, they dissolved sodium into an organic mixture (biphenyl [Bp] and dimethoxyethane [DME]) to achieve a Na-Bp-DME liquid anode. This liquid anode possessed a low potential of 0.09 V vs Na and high conductivity of 1.2×10^{-2} S cm^{-1} at room temperature. This liquid anode had a high degree of safety because it reacted with water in a much milder way than Na metal. Unlike liquid K-Na alloy, the Na-Bp-DME liquid anode cannot be used in liquid electrolyte. Instead, a solid electrolyte has to be used with this type of liquid anode. A prototype Na-S battery (Na_2S|| BASE||Na-BP-DME) was assembled using Na-Bp-DME as anode and Na-β″-Al_2O_3 solid electrolyte (BASE) as the solid electrolyte, which sustained over 3500 cycles without measurable capacity loss at room temperature. Compared to the solid-state K metal anode, the liquid K-based anodes generally are dendrite-free and have a stable SEI, fast and facile K diffusion and reaction kinetics, and easily-relaxed stresses due to the good fluidity of the liquid. Based on this concept of the liquid alkali metal organic anode, Yichun Lu et al developed a potassium biphenyl (BpK) liquid anode and applied it in the K-O_2 battery, which showed high safety, high rate performance and long lifespan with superior performance (3000 cycles and CE of 99.84%).[129] The superior performance obtained with BpK liquid anode can be attributed to the advantages of the good fluidity of the liquid. Compared to the solid-state K metal anode, the liquid state K-based anodes generally are dendrite-free and have a stable SEI, fast and facile K diffusion and reaction kinetics, and easily relaxed stresses that are induced during cycles of plating/stripping. So far, only a few reports on K-based batteries have used liquid K-based anodes, but they have demonstrated their great potential. Therefore, we encourage the scientific research community to pay more attention to this field and design more potassium-sulfur batteries using K-based anodes.

3.3 | Electrolytes

For current K-S batteries, the electrolytes employed include liquid electrolytes (ether-based and ester-based electrolytes) and solid-state electrolytes (SSEs) (polymer-based and inorganic-based SSEs). As an essential component of batteries, the electrolytes play vital roles in transporting ions and stabilizing electrode/electrolyte interfaces to support long operation life. Thus, they are important for optimizing the battery performance and promoting its practical applications.

3.3.1 | Liquid electrolyte

For liquid-electrolyte based K-S batteries, the shuttle effect, caused by the free migration of dissolved polysulfide during cell operation, is a crucial challenge for achieving high energy density and long cycling life, In particular, these dissolved long-chain redox species (K_2S_n, $4 \le n \le 8$) can be reduced chemically when diffusing to the anode material to form lower-order polysulfides (K_2S_n, $1 \le n \le 3$) and then diffuse back to the sulfur cathode to be re-oxidized. These parasitic reactions have a considerable negative impact on K-S batteries, including the irreversible consumption of active material at the cathode, the formation of a passivation layer on the anode material, and electrolyte depletion because of attacks by the highly active polysulfide species. Nevertheless, due to the wide range of polar/nonpolar characteristics of sulfur and its polysulfides, it is difficult to choose electrolytes with perfect insolubility for all the polysulfide intermediates. For a specific electrolyte system, understanding the solid-solution properties of polysulfides is highly necessary for explaining and optimizing battery performance.

Hwang and his co-workers have synthesized a series of K_2S_x ($1 \le x \le 6$) polysulfides and studied their solubility in diethylene glycol dimethyl ether (DEGDME).[39] Unlike lithium polysulfide, K_2S_x with short chains ($x < 5$) cannot be dissolved in DEGDME, while the ones with long chains ($5 \le x$) are completely dissolved with a dark brown appearance. Further, Gu et al thoroughly investigated the properties of K_2S_x ($1 \le x \le 3$) in potassium bis-(fluorosulfonyl)imide (KFSI)-dimethoxyethane (DME) electrolyte, including their solubility, the related disproportionation reactions, and the chemical compatibility between KFSI and the polysulfides.[62] Specifically, they quantified the solubility of K_2S_3 and K_2S_2 in DME solvent and showed that their solubilities are as low as 71.4 mg 100 g^{-1} and 12.6 mg 100 g^{-1} (Table 2), respectively. Despite its low solubility in DME, K_2S_3 can still produce yellowish soluble polysulfide (Figure 7A) species, which consist of detectable S_5^{2-}, S_4^{2}, and $S_3^{\bullet-}$ via UV-Vis analysis (Figure 7B). As S_5^{2-} will be further disproportionated into S_6^{2-} and S_4^{2-}, this indicates that K_2S_3 is disproportionated into K_2S_6, K_2S_4, K_2S_5, and likely K_2S and K_2S_2. When there was a salt (KFSI) presented, however, the dissolution of K_2S_3 was suppressed due to the common ionic effect caused by the increased K^+ concentration (Figure 7B). In addition, they also demonstrated that the FSI^- anion is stable in the presence of K_2S_3 via nuclear magnetic resonance (NMR) spectroscopy, confirming the chemical stability of KFSI-DME electrolyte in K-S batteries.

In addition to investigating the basic properties of polysulfides in a specific electrolyte, researchers have tried to incorporate redox additives into the electrolyte to achieve high energy density for K-S batteries. Lai et al added a copper (II) salt (copper trifluoromethanesulfonate, $Cu[TFS]_2$) in potassium trifluoromethanesulfonate (KTFS) in the 1-methylimidazole (Me-Im) system as catalyst to promote the reduction kinetics of K_2S_3 to K_2S, aiming to achieve a high energy density. The reason why they chose Me-Im was to maximize the solubility of polysulfide.[37] $Cu(TFS)_2$ can be readily dissolved in Me-Im and forms the Me-Im-solvated Cu^{2+} active species. Coupled with a stable potassium biphenyl anode (BpK), the BpK-S battery with Cu^{2+} (denoted as "S/Cu^{2+}") exhibited dramatically increased performance compared with a BpK-S cell (denoted as "S"), and a BpK-Cu^{2+} cell (denoted as "Cu^{2+}"). This is ascribed to the complete reduction of S_3^{2-} to S^{2-}. An obvious higher average cell voltage for "S/Cu^{2+}" than for "Cu^{2+}" and "S" further proves the enhanced reduction kinetics of the change from S_3^{2-} to S^{2-}. They also revealed the mechanism responsible for the remarkable performance improvement in the KTFS- Me-Im- Cu^{2+} system. On replacing Me-Im with other solvents, such as diglyme (DG) and dimethyl sulfoxide (DMSO), the effectiveness of the Cu^{2+} catalyst was much reduced, suggesting that the solvation of Me-Im molecules (with imidazole nitrogen atoms) around Cu^{2+} ions is essential for catalyzing the formation of K_2S.

Other electrolytes, including 1.0 M $KClO_4$ in tetraethylene glycol dimethyl ether (TEGDME),[36] potassium trifluoromethanesulfonate (KCF_3SO_3)/TEGDME,[51] and KPF_6 in ethylene carbonate (EC)/dimethyl carbonate (DEC),[39,60] have been tried in K-S systems. As summarized in Table 3, both ether-based and carbonate-based electrolytes have been used in K-S batteries, and organic potassium salts are more widely utilized than inorganic ones. Compared with carbonate-based electrolytes, ether-based electrolytes are reported to possess better compatibility with K metal anodes, thus inspiring high motivation to employ them for high-performance K-S systems.[17]

Nevertheless, the investigation of liquid electrolytes for K-S batteries is still at an early stage, more efforts to obtain a detailed understanding of the chemistry of polysulfides in solution, strategies for confronting intermediate shuttling, and the exploitation of novel systems (eg, ionic-liquid, concentrated electrolytes) should be undertaken in the future.

3.3.2 | Solid electrolyte

SSEs present a solution for high energy density in high-safety alkaline metal-based sulfur batteries that benefit from their ability to obstruct the polysulfide shuttle and block metal dendrites. Notwithstanding that there are not as many reports on SSEs for K^+ as for Li^+, progress has been witnessed in recent years. A pioneering work was conducted in Goodenough's group, where they employed polymer-gel electrolyte with cross-linked poly (methyl methacrylate) (PMMA) in potassium batteries with polyaniline as cathode.[131] Compared with liquid electrolyte (0.8 M KPF_6 in EC/DEC/FEC), the potassium battery with the polymer-gel electrolyte exhibited much improved cycling stability, as well as CE, implying the important role of the SSE in stabilizing the electrode/electrolyte interfaces during cycling. Xiao et al reported

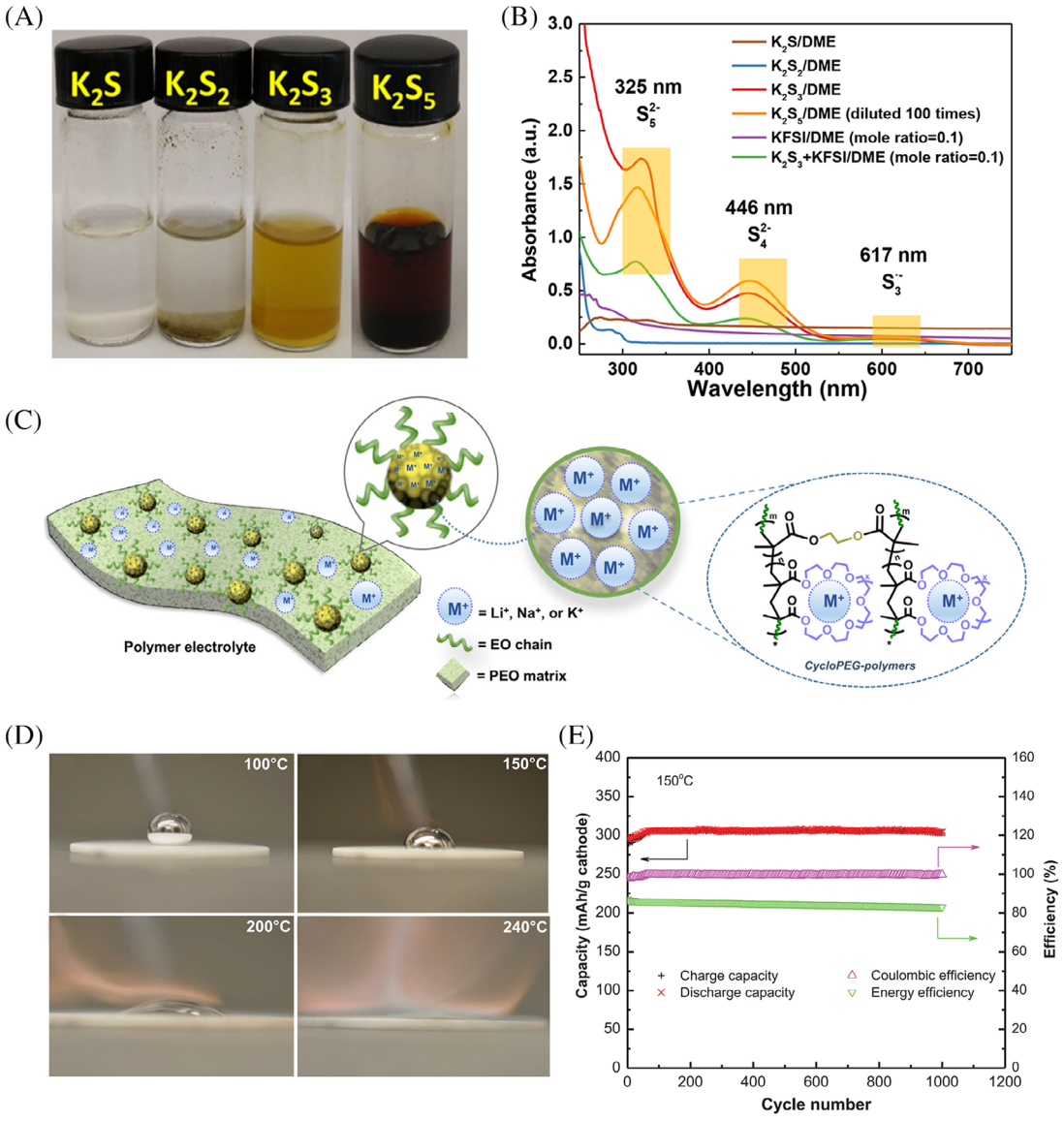

FIGURE 7 A, Images of K_2S_x (x = 1-3, 5) dissolved in DME. B, UV-Vis spectra for K_2S_x (x = 1-3, 5) in different solutions. Reproduced with permission. Copyright 2018, American Chemical Society.[62] C, Schematic illustration of polymer electrolyte with the structure of the star polymer. Reproduced with permission. Copyright 2019, Elsevier.[130] D, Wettability of liquid K on untreated K-BASE. E, Cycling performance of a K-S cell at 150°C[43]

the synthesis of a tailor-made star polymer via cation template-assisted cyclopolymerization, which was composed of cross-linked cores containing pseudo-crown ether cavities and polyethylene oxide (PEO) arms (Figure 7C).[130] Thus, it showed universal conductivity for alkali ions (Li^+, Na^+, K^+). Their ionic conductivities in different alkaline metal-ion batteries were measured, and the optimized value for K^+ was found to reach 9.84×10^{-4} S cm^{-1} at 80°C. Feng's group reported a room temperature poly(propylene carbonate) (PPC)-KFSI based SSE for all-solid state PIBs.[132] The PPC-KFSI based SSE was fabricated by first casting a mixed tetrahydrofuran solution of PPC and KFSI onto cellulose nonwoven membranes and then evaporating the solvent. When demonstrated in an all-solid-state potassium battery based on a 3,4,9,10-perylene-tetracarboxylicacid-dianhydride (PTCDA) cathode, the PPC-KFSI based SSE showed high ionic conductivity of 1.36×10^{-5} S cm^{-1} at ambient temperature.

In addition to polymer-based SSE, inorganic based electrolytes are also being exploited. Feng's group employed a $K_2Fe_4O_7$ ceramic pellet as SSE in a potassium metal battery using Prussian blue as cathode.[132] $K_2Fe_4O_7$ was synthesized under hydrothermal conditions, and it featured a 3D open framework for K^+ transportation. It manifested many advantages in potassium metal batteries, including a K^+ ion conductivity of 5×10^{-2} S cm^{-1} at room temperature, a wide voltage window up to 5 V vs K/K^+, and chemical stability toward potassium metal. As a result, the all-solid-state potassium metal battery based on the prepared $K_2Fe_4O_7$ SSE exhibited remarkable performance with an impressive high rate capability of 250 C (1 C = 87 mA h g^{-1}). Lu and his co-workers employed K-BASE electrolyte for moderate-temperature K-S batteries.[43] The components for the K-BASE sample included 91 wt % K-β''-Al_2O_3, 8.4 wt% K-β-Al_2O_3, and 0.6 wt% ZrO_2. The wettability test showed that potassium was capable of good wetting performance on K-BASE at temperatures higher than 150°C (Figure 7D). It also showed very good conductive properties, with high conductivity around 0.056 and 0.01 S cm^{-1} at 300 and 150°C, respectively. When tested in a K-S cell constructed with a potassium polysulfide catholyte paired with molten potassium at 150°C, remarkable cycling stability over 1000 cycles with negligible degradation was achieved (Figure 7E). This work is inspiring for the future development of K-S full cells to work at a moderate temperature, such as 150°C.

4 | OUTLOOK AND PERSPECTIVES

Overall, K-S batteries are attracting increasing attention as a high-energy-density and low-cost alternative to current LIBs. Although some efforts have been made in terms of cathode design, anode protection, and electrolyte optimization, and reasonable progress has been witnessed, the study of K-S batteries is still at a very initial stage. Advances in our understanding of the potassiation mechanism of sulfur, enhancement of the reaction kinetics, relief of the shuttle effect and solutions to the safety hazard would be highly desirable. In addition, constructing evaluation parameters suitable for industrial purposes is essential to ensure that new developments palpably contribute to make the K-S technology commercially relevant. This requirement looks too harsh for such a new technology, but it is reasonable and may be compulsory to a certain degree, as its Li-S counterpart is undergoing such a transition to realize its practical promise. With respect to advancing the development of K-S batteries, we would like to share our perspectives on possible future directions in this area:

4.1 | Developing advanced cathode materials

The requirements for an ideal cathode for K-S batteries include high conductivity, high sulfur loading and utilization, good trapping ability for polysulfides, and fast reduction kinetics for the transition from K_2S_3 to K_2S. Current strategies for increasing the conductivity are focused on conductive framework design, such as with carbon coating, porous carbon loading, and so forth. Future directions might change to modify sulfur to increase its intrinsic conductivity, such as by alloying sulfur with selenium (Se) or tellurium (Te). They belong to the same chalcogen group as sulfur, but possess much higher electrical conductivity (10^{-3} for Se vs 10^{-27} S m^{-1} for S at room temperature). Inspired results have been obtained in Li-SeS_x and Na-SeS_x systems, where a small amount of selenium substitution in sulfur can significantly improve its sodiation and lithiation kinetics.[133,134] Moreover, our group members have demonstrated the promise of the K-Se battery.[135] It is believed that exploring the K-SeS_x system would offer more opportunities for disentangling the various factors that may be responsible for holding back the "pure" K-S system.[17] Other important aspects of performance to be considered are the sulfur loading/utilization, and the polysulfide trapping capability, which impose special requirements on the sulfur host design. In the Li-S battery, the chemical interactions between sulfur and its host materials have been extensively studied, and the results indicate that the surface functionality, intrinsic polarity, electro-/nucleophilicity, and/or redox potential play important roles in determining the strength of the interaction. Among the

reported sulfur hosts, metal-organic frameworks (MOFs) and nonstoichiometric metal chalcogenides have been calculated to possess the highest binding energy toward lithium sulfide,[136,137] which should be also paid special attention in K-S systems. Finally, a catalytic cathode with the functionality to promote the reduction kinetics for the K_2S_3 to K_2S reaction should be developed in the future. A series of catalysts have been demonstrated to be efficient enough to enhance the kinetics of the reaction from soluble polysulfides to insoluble S (in the charge process) or sulfide (in the discharge process) in Li-S and Na-S systems, such as platinum (Pt), gold (Au), cobalt (Co), and metal oxides/sulfides/nitrides.[29,138-143] Their catalytic effects in K-S batteries are waiting to be discovered. Notably, all the proposed strategies require an in-depth understanding of the mechanism. Recently, in situ characterization technologies such as in situ infrared spectroscopy,[144] in situ Raman spectraoscopy,[145] in situ electron microscopy,[146] in situ synchrotron powder diffraction,[147,148] in situ synchrotron X-ray powder diffraction,[149] and so forth have been employed and proved to be efficient at revealing the mechanisms behind the electrochemical reactions (including the electrode reactions, electrolyte decomposition, SEI formation and regeneration, etc). Therefore, future research should rely more on these technologies to solve the current issues with K-S batteries.

4.2 | Building a stable potassium anode

The prerequisite for a stable potassium anode is the formation of a stable SEI layer on its surface, which impedes any further reaction between the potassium and the electrolyte, and avoids dendrite growth. We still know little about potassium's SEI layer, however, owing to the super-activity of potassium, which imposes difficulties for observations and characterizations. Thus, the urgent task here is to understand the structure and chemistry of the SEI for potassium. Recently, by virtue of cryo-electron microscopy (cryo-EM), researchers have observed solid-liquid interfaces and dendrites on lithium anodes, and this technique is expected to be used for the observation of SEI layers in K-S batteries.[150,151] Key questions, such as the detailed components of the SEI layer, its evolution with the working potentials, the core component passivating the metal, and so forth, should be answered. Based on a fundamental understanding of the SEI layer in K-S batteries, efficient strategies can be designed and applied, including, but not limited to, artificial SEI layer construction, host architecture design, the application of concentrated electrolyte, self-healing, and so forth. In addition, multiscale modeling can be used to interpret experimental results and provide predictions to enable further experimental optimization, targeted at efficiently and reliably realizing a stable potassium anode for advancing progress toward a practical battery.

4.3 | Electrolyte optimization

Various electrolytes, including liquid-electrolytes, polymer-based electrolytes, and inorganic-solid state electrolytes, have been employed in the K-S system, although reports on electrolyte optimizations are still limited. Nevertheless, the electrolyte plays a vital role in overcoming the polysulfide dissolution and shuttle problem, which should be paid much more attention for the development of practical K-S batteries. For now, the liquid-electrolyte based K-S battery is still the most promising one owing to the mature development of various liquid electrolytes. Nevertheless, dissolution of polysulfides, the shuttle effect, and safety concerns related to flammability are highly challenging for liquid electrolytes. Compared with conventional electrolytes (carbonate-based and ether-based electrolytes), ionic-liquid (IL)-based electrolytes have been attracting special attention due to their unique solvation behavior. In Li-S batteries, certain IL-based liquid electrolytes have been found to suppress the solubility of all the redox-active species while maintaining acceptable ionic conductivity.[152] The cationic/anionic dependence of the solubility of S_8 and polysulfides have also been revealed.[153] As a result, it is possible to custom-make IL electrolytes with desirable performance, which should be highly promising for K-S batteries. Adding redox mediators (RMs) has been proved to be another efficient approach to achieving high-performance K-S batteries, as they can control the precipitation of K_2S on the cathode host on discharge and lower the overpotential for its oxidation on charge.[137,154] Generally, they are molecules with reversible redox couples that undergo electrochemical reduction or oxidation at the electrode and diffuse to the active material. Thus, with the presence of RMs, uncontacted active material can even be electrochemically coupled to the electrode surface, thus avoiding the formation of "dead" active materials. In addition, safety concerns about conventional organic electrolytes remains a critical factor in determining the practical applications of large-scale rechargeable batteries. It is an especially severe problem in the development of potassium-based batteries, since K metal is extremely active toward oxygen and water. In this regard, employing nonflammable electrolytes is highly attractive and highly recommended. Recently, Liu et al reported a low-cost and fire-retardant phosphate-based electrolyte (potassium bis(fluorosulfonyl)imide in triethyl

phosphate) for rechargeable PIBs, which manifested excellent performance with a moderate concentration.[155] Inspired by this work, more efforts should be directed toward the design of low-cost and nonflammable electrolyte systems with fire-retardant solvents in the future to make the K-S system a reality.

4.4 | Practical cell parameters

To obtain high-energy-density metal-sulfur batteries for practical use, several cell parameters need to be kept in the practical range, including high sulfur loading, a low electrolyte/sulfur (E/S) ratio, an ultrathin metal anode, and so forth. Recently, the Li-S research community has realized the importance and necessity of considering the practical cell parameters in the pursuit of practical high-energy-density Li-S batteries and deliberately moved in this direction. In this context, Manthiram et al has proposed the five 5 seconds for high energy Li-S batteries, which are sulfur loading >5 mg cm^{-2}, carbon content <5%, E/S ratio <5 mL mg^{-1}, E/C ratio <5 mL (mA h) $^{-1}$, and the negative to positive electrode ratio (N/P) ratio <5 in pouch-type cells. Unfortunately, state-of-the-art K-S batteries with decent performance are obtained with mild cell parameters (ie, low sulfur content of 30-70 wt %, a low sulfur loading of <1.2 mg cm^{-2}, and high electrolyte/sulfur ratios of over 48 μL mg^{-1}) rather than practical cell parameters such as the five 5 seconds parameters. Therefore, it is likely that the performance of the K-S battery will be worse when practical cell parameters are used. Due to the inherent disadvantages of the K-S battery, such as the poor solubility of short chain potassium polysulfides, large volume expansion during electrochemical redox reactions, and the high chemical activity of K metal, the K-S battery faces more severe challenges under practical cell parameters. For example, the high sulfur loading and sulfur content mean that there will be less conductive carbon in the cathode. The low content of carbon substrate leads to poor conductive contact and weak confinement of sulfur within the carbon substrate, causing the loss of active material and capacity decay. The use of ultrathin K metal anode means that nearly the entire K metal anode would experience stripping/plating during each cycle. The huge volume changes of K metal anode induce severe cracking and reforming of the SEI on the K metal surface, making problems such as low CE and short lifespan more pronounced. The use of lean electrolyte may result in insufficient wetting of the positive electrode, resulting in low sulfur utilization, low capacity, and short cycle life. To address these challenges, new design guidelines may be required for the cathode, electrolyte, and anode. For example, binder is widely used in current K-S batteries to fix the active materials, and some designs focusing on binder have been proposed to improve the performance of K-S batteries.[39] Binder as a nonactive material, however, needs a large amount of extra electrolyte to overcome the wettability and ion diffusion problems. Therefore, binder-free cathode is more favorable with practical cell parameters (eg, use of lean electrolyte) as it reduces the weight of both the electrolyte and the binder. Some recent K-S batteries have adopted two-layer separators to impede the polysulfide shuttle from the cathode to the anode.[62] The use of additional separator will lead to an increase in the weight of the nonactive substances, however, resulting in a decrease in energy density. Therefore, many design criteria under mild conditions (ie, flooded electrolyte, low sulfur loading, thick anode, etc) are no longer applicable to battery design under practical conditions. Future research should consider more new design options. For example, polysulfides dispersed on a self-supporting conductive substrate is a promising cathode design, as it has high sulfur loading and uniform sulfur dispersion, and it eliminates binders and current collectors and thus improves the mass ratio of active materials in the whole battery.[156,157] In order to adapt to the practical parameter of lean electrolyte, high wettability, high conductivity, and moderate specific surface are key factors for cathode design. Although the current research on the K-S battery is still in its early stage and is still far from being practical, achieving high performance under practical conditions is a challenge that K-S batteries must confront and overcome on the road to their practical use.

ACKNOWLEDGMENTS

X. Z., R. W., and Z. Q. would like to acknowledge the China Postdoctoral Science Foundation (2019M663047), the Science and Technology Innovation Commission of Shenzhen (20180123 and JCYJ20190808173815205), the Natural Science Foundation of Guangdong Province (2019A1515012111), the National Natural Science Foundation of China (51804199), and the Shenzhen Science and Technology Program (KQTD20180412181422399). Y. L. and Z. G. would like to acknowledge the Australian Research Council for its support through a Discovery project (DP200101862), a Linkage project (LP160101629), and a Discovery Early Career Researcher Award Fellowship (DE190100082).

ORCID

Xinyu Zhao https://orcid.org/0000-0002-1098-5670
Yan Lu https://orcid.org/0000-0002-4110-5285

Renheng Wang https://orcid.org/0000-0003-0946-7830
Zaiping Guo https://orcid.org/0000-0003-3464-5301

REFERENCES

1. Liu Y, Zhu Y, Cui Y. Challenges and opportunities towards fast-charging battery materials. *Nat Energy*. 2019;4:540-550.
2. Li M, Lu J, Ji X, et al. Design strategies for nonaqueous multivalent-ion and monovalent-ion battery anodes. *Nat Rev Mater*. 2020;5:1-19.
3. Cano ZP, Banham D, Ye S, et al. Batteries and fuel cells for emerging electric vehicle markets. *Nat Energy*. 2018;3:279-289.
4. Dunn B, Kamath H, Tarascon J-M. Electrical energy storage for the grid: a battery of choices. *Science*. 2011;334:928-935.
5. Goodenough JB. Evolution of strategies for modern rechargeable batteries. *Acc Chem Res*. 2013;46:1053-1061.
6. Grey C, Tarascon J. Sustainability and in situ monitoring in battery development. *Nat Mater*. 2017;16:45-56.
7. Cao Y, Li M, Lu J, Liu J, Amine K. Bridging the academic and industrial metrics for next-generation practical batteries. *Nat Nanotechnol*. 2019;1:200–207.
8. Chung SH, Manthiram A. Current status and future prospects of metal-sulfur batteries. *Adv Mater*. 2019;31:1901125.
9. Choi JW, Aurbach D. Promise and reality of post-lithium-ion batteries with high energy densities. *Nat Rev Mater*. 2016;1:1-16.
10. Muldoon J, Bucur CB, Gregory T. Quest for nonaqueous multivalent secondary batteries: magnesium and beyond. *Chem Rev*. 2014;114:11683-11720.
11. Scrosati B, Hassoun J, Sun Y-K. Lithium-ion batteries. A look into the future. *Energy Environ Sci*. 2011;4:3287-3295.
12. Seh ZW, Sun Y, Zhang Q, Cui Y. Designing high-energy lithium-sulfur batteries. *Chem Soc Rev*. 2016;45:5605-5634.
13. Yang Y, Zheng G, Cui Y. Nanostructured sulfur cathodes. *Chem Soc Rev*. 2013;42:3018-3032.
14. Evers S, Nazar LF. New approaches for high energy density lithium-sulfur battery cathodes. *Acc Chem Res*. 2013;46:1135-1143.
15. Whittingham MS. Lithium batteries and cathode materials. *Chem Rev*. 2004;104:4271-4302.
16. Li G, Wang S, Zhang Y, Li M, Chen Z, Lu J. Revisiting the role of polysulfides in lithium-sulfur batteries. *Adv Mater*. 2018;30:1705590.
17. Ding J, Zhang H, Fan W, Zhong C, Hu W, Mitlin D. Review of emerging potassium-sulfur batteries. *Adv Mater*. 2020;32:1908007.
18. Eftekhari A. Lithium batteries for electric vehicles: from economy to research strategy. *ACS Sustain Chem Eng*. 2019;7:5602-5613.
19. Yao Y-FY, Kummer J. Ion exchange properties of and rates of ionic diffusion in beta-alumina. *J Inorg Nucl Chem*. 1967;29:2453-2475.
20. Kummer J, Weber N. US Patent; 1969.
21. Wen Z, Hu Y, Wu X, Han J, Gu Z. Main challenges for high performance NAS battery: materials and interfaces. *Adv Funct Mater*. 2013;23:1005-1018.
22. Sudworth J, Tiley A. *Sodium Sulphur Battery*. London: Chapman and Hall; 1985.
23. Manthiram A, Yu X. Ambient temperature sodium-sulfur batteries. *Small*. 2015;11:2108-2114.
24. Bito A. Overview of the sodium-sulfur battery for the IEEE Stationary Battery Committee. *IEEE Power Engineering Society General Meeting, 2005*. San Francisco, CA: IEEE; 2005:1232-1235.
25. Berbano SS, Seo I, Bischoff CM, Schuller KE, Martin SW. Formation and structure of $Na_2S + P_2S_5$ amorphous materials prepared by melt-quenching and mechanical milling. *J Non Cryst Solids*. 2012;358:93-98.
26. Wang YX, Zhang B, Lai W, et al. Room-temperature sodium-sulfur batteries: a comprehensive review on research progress and cell chemistry. *Adv Energy Mater*. 2017;7:1602829.
27. Hong X, Mei J, Wen L, et al. Nonlithium metal-sulfur batteries: steps toward a leap. *Adv Mater*. 2019;31:1802822.
28. Zhu J, Zou J, Cheng H, Gu Y, Lu Z. High energy batteries based on sulfur cathode. *Energy Environ Sci*. 2019;4:345-359.
29. Wang N, Wang Y, Bai Z, et al. High-performance room-temperature sodium-sulfur battery enabled by electrocatalytic sodium polysulfides full conversion. *Energy Environ Sci*. 2020;13:562–570.
30. Yan Z, Xiao J, Lai W, et al. Nickel sulfide nanocrystals on nitrogen-doped porous carbon nanotubes with high-efficiency electrocatalysis for room-temperature sodium-sulfur batteries. *Nat Commun*. 2019;10:1-8.
31. Hwang TH, Jung DS, Kim J-S, Kim BG, Choi JW. One-dimensional carbon-sulfur composite fibers for Na-S rechargeable batteries operating at room temperature. *Nano Lett*. 2013;13:4532-4538.
32. Li Y, Zhang L, Liu S, et al. Original growth mechanism for ultra-stable dendrite-free potassium metal electrode. *Nano Energy*. 2019;62:367-375.
33. Yan Z, Liang Y, Xiao J, et al. A high-kinetics sulfur cathode with a highly efficient mechanism for superior room-temperature Na-S batteries. *Adv Mater*. 2020;32:1906700.
34. Zhang W, Liu Y, Guo Z. Approaching high-performance potassium-ion batteries via advanced design strategies and engineering. *Sci Adv*. 2019;5:eaav7412.
35. Yabuuchi N, Kubota K, Dahbi M, Komaba S. Research development on sodium-ion batteries. *Chem Rev*. 2014;114:11636-11682.
36. Zhao Q, Hu Y, Zhang K, Chen J. Potassium-sulfur batteries: a new member of room-temperature rechargeable metal-sulfur batteries. *Inorg Chem*. 2014;53:9000-9005.
37. Lai N-C, Cong G, Lu Y-C. A high-energy potassium-sulfur battery enabled by facile and effective imidazole-solvated copper catalysts. *J Mater Chem A*. 2019;7:20584-20589.
38. Liu Y, Wang W, Wang J, et al. Sulfur nanocomposite as a positive electrode material for rechargeable potassium-sulfur batteries. *Chem Commun*. 2018;54:2288-2291.
39. Hwang J-Y, Kim HM, Sun Y-K. High performance potassium-sulfur batteries based on a sulfurized polyacrylonitrile cathode and polyacrylic acid binder. *J Mater Chem A*. 2018;6:14587-14593.
40. Lei K, Wang C, Liu L, et al. A porous network of bismuth used as the anode material for high-energy-density potassium-ion batteries. *Angew Chem Int Ed*. 2018;57:4687-4691.
41. Tang X, Zhou D, Li P, et al. MXene-based dendrite-free potassium metal batteries. *Adv Mater*. 2020;32:1906739.

42. Wang L, Bao J, Liu Q, Sun C-F. Concentrated electrolytes unlock the full energy potential of potassium-sulfur battery chemistry. *Energy Storage Mater*. 2019;18:470-475.
43. Lu X, Bowden ME, Sprenkle VL, Liu J. A low cost, high energy density, and long cycle life potassium-sulfur battery for grid-scale energy storage. *Adv Mater*. 2015;27:5915-5922.
44. Wu X, Leonard DP, Ji X. Emerging non-aqueous potassium-ion batteries: challenges and opportunities. *Chem Mater*. 2017;29:5031-5042.
45. Rajagopalan R, Tang Y, Ji X, Jia C, Wang H. Advancements and challenges in potassium ion batteries: a comprehensive review. *Adv Funct Mater*. 2020;30:1909486.
46. Kubota K, Dahbi M, Hosaka T, Kumakura S, Komaba S. Towards K-ion and Na-ion batteries as "beyond Li-ion". *Chem Rec*. 2018;18:459-479.
47. Matsuura N, Umemoto K, Takeuchi Z. Standard potentials of alkali metals, silver, and thallium metal/ion couples in N,N′-dimethylformamide, dimethyl sulfoxide, and propylene carbonate. *Bull Chem Soc Jpn*. 1974;47:813-817.
48. Lei K, Li F, Mu C, et al. High K-storage performance based on the synergy of dipotassium terephthalate and ether-based electrolytes. *Energy Environ Sci*. 2017;10:552-557.
49. Okoshi M, Yamada Y, Komaba S, Yamada A, Nakai H. Theoretical analysis of interactions between potassium ions and organic electrolyte solvents: a comparison with lithium, sodium, and magnesium ions. *J Electrochem Soc*. 2017;164:A54-A60.
50. Medenbach L, Adelhelm P. Cell concepts of metal-sulfur batteries (metal=Li, Na, K, Mg): strategies for using sulfur in energy storage applications. In: Eichel R-A, ed. *Electrochemical Energy Storage*. Switzerland : Springer; 2019:101-125.
51. Yu X, Manthiram A. A reversible nonaqueous room-temperature potassium-sulfur chemistry for electrochemical energy storage. *Energy Storage Mater*. 2018;15:368-373.
52. Adams RA, Varma A, Pol VG. Carbon anodes for nonaqueous alkali metal-ion batteries and their thermal safety aspects. *Adv Energy Mater*. 2019;9:1900550.
53. Fang R, Xu J, Wang D-W. Covalent fixing of sulfur in metal-sulfur batteries. *Energy Environ Sci*. 2020;13:432-471.
54. Xin S, Gu L, Zhao N-H, et al. Smaller sulfur molecules promise better lithium–sulfur batteries. *J Am Chem Soc*. 2012;134:18510-18513.
55. He H, Huang D, Gan Q, et al. Anion vacancies regulating endows MoSSe with fast and stable potassium ion storage. *ACS Nano*. 2019;13:11843-11852.
56. Zhang L, Zhang B, Wang C, et al. Constructing the best symmetric full K-ion battery with the NASICON-type $K_3V_2(PO_4)_3$. *Nano Energy*. 2019;60:432-439.
57. Yang F, Gao H, Hao J, et al. Yolk-shell structured FeP@C nanoboxes as advanced anode materials for rechargeable lithium−/potassium-ion batteries. *Adv Funct Mater*. 2019;29:1808291.
58. Chung WJ, Griebel JJ, Kim ET, et al. The use of elemental sulfur as an alternative feedstock for polymeric materials. *Nat Chem*. 2013;5:518-524.
59. Zhu J, Zhu P, Yan C, Dong X, Zhang X. Recent progress in polymer materials for advanced lithium-sulfur batteries. *Prog Polym Sci*. 2019;90:118-163.
60. Xiong P, Han X, Zhao X, et al. Room-temperature potassium–sulfur batteries enabled by microporous carbon stabilized small-molecule sulfur cathodes. *ACS Nano*. 2019;13:2536-2543.
61. Yu X, Manthiram A. Capacity enhancement and discharge mechanisms of room-temperature sodium-sulfur batteries. *ChemElectroChem*. 2014;1:1275-1280.
62. Gu S, Xiao N, Wu F, Bai Y, Wu C, Wu Y. Chemical synthesis of K_2S_2 and K_2S_3 for probing electrochemical mechanisms in K-S batteries. *ACS Energy Lett*. 2018;3:2858-2864.
63. Lindberg D, Backman R, Hupa M, Chartrand P. Thermodynamic evaluation and optimization of the (Na+ K+ S) system. *J Chem Thermodyn*. 2006;38:900-915.
64. Pringle DL. *The Nature of the Polysulfide Anion*. Ames, IA: Iowa State University; 1967.
65. Cao R, Xu W, Lv D, Xiao J, Zhang JG. Anodes for rechargeable lithium-sulfur batteries. *Adv Energy Mater*. 2015;5:1402273.
66. Ma S, Zuo P, Zhang H, et al. Iodine-doped sulfurized polyacrylonitrile with enhanced electrochemical performance for room-temperature sodium/potassium sulfur batteries. *Chem Commun*. 2019;55:5267-5270.
67. Ma R, Fan L, Wang J, Lu B. Confined and covalent sulfur for stable room temperature potassium-sulfur battery. *Electrochim Acta*. 2019;293:191-198.
68. Hwang J-Y, Kim HM, Yoon CS, Sun Y-K. Toward high-safety potassium–sulfur batteries using a potassium polysulfide catholyte and metal-free anode. *ACS Energy Lett*. 2018;3:540-541.
69. Li Z, Wu HB, Lou XW. Rational designs and engineering of hollow micro-/nanostructures as sulfur hosts for advanced lithium-sulfur batteries. *Energy Environ Sci*. 2016;9:3061-3070.
70. Li Z, Zhang J, Guan B, Wang D, Liu L-M, Lou XW. A sulfur host based on titanium monoxide@carbon hollow spheres for advanced lithium-sulfur batteries. *Nat Commun*. 2016;7:1-11.
71. Wang J, He YS, Yang J. Sulfur-based composite cathode materials for high-energy rechargeable lithium batteries. *Adv Mater*. 2015;27:569-575.
72. Xu Z-L, Kim J-K, Kang K. Carbon nanomaterials for advanced lithium sulfur batteries. *Nano Today*. 2018;19:84-107.
73. Ji X, Lee KT, Nazar LF. A highly ordered nanostructured carbon-sulphur cathode for lithium-sulphur batteries. *Nat Mater*. 2009;8:500-506.
74. Jayaprakash N, Shen J, Moganty SS, Corona A, Archer LA. Porous hollow carbon@sulfur composites for high-power lithium-sulfur batteries. *Angew Chem Int Ed*. 2011;50:5904-5908.
75. He G, Ji X, Nazar L. High "C" rate Li-S cathodes: sulfur imbibed bimodal porous carbons. *Energy Environ Sci*. 2011;4:2878-2883.
76. Schuster J, He G, Mandlmeier B, et al. Spherical ordered mesoporous carbon nanoparticles with high porosity for lithium-sulfur batteries. *Angew Chem Int Ed*. 2012;51:3591-3595.
77. Zhang Q, Wang Y, Seh ZW, Fu Z, Zhang R, Cui Y. Understanding the anchoring effect of two-dimensional layered materials for lithium-sulfur batteries. *Nano Lett*. 2015;15:3780-3786.
78. Zhou G, Yin L-C, Wang D-W, et al. Fibrous hybrid of graphene and sulfur nanocrystals for high-performance lithium–sulfur batteries. *ACS Nano*. 2013;7:5367-5375.

79. Liang J, Sun Z-H, Li F, Cheng H-M. Carbon materials for Li-S batteries: functional evolution and performance improvement. *Energy Storage Mater*. 2016;2:76-106.
80. Ma L, Zhuang HL, Wei S, et al. Enhanced Li-S batteries using amine-functionalized carbon nanotubes in the cathode. *ACS Nano*. 2016;10:1050-1059.
81. Zhou G, Paek E, Hwang GS, Manthiram A. Long-life Li/polysulphide batteries with high sulphur loading enabled by lightweight three-dimensional nitrogen/sulphur-codoped graphene sponge. *Nat Commun*. 2015;6:1-11.
82. Demir-Cakan R, Morcrette M, Nouar F, et al. Cathode composites for Li-S batteries via the use of oxygenated porous architectures. *J Am Chem Soc*. 2011;133:16154-16160.
83. Borchardt L, Oschatz M, Kaskel S. Carbon materials for lithium sulfur batteries—ten critical questions. *Chem A Eur J*. 2016;22:7324-7351.
84. Hou TZ, Xu WT, Chen X, Peng HJ, Huang JQ, Zhang Q. Lithium bond chemistry in lithium-sulfur batteries. *Angew Chem Int Ed*. 2017;56:8178-8182.
85. Wang J, Yang J, Xie J, Xu N. A novel conductive polymer-sulfur composite cathode material for rechargeable lithium batteries. *Adv Mater*. 2002;14:963-965.
86. Song M-K, Zhang Y, Cairns EJ. A long-life, high-rate lithium/sulfur cell: a multifaceted approach to enhancing cell performance. *Nano Lett*. 2013;13:5891-5899.
87. Manthiram A, Fu Y, Chung S-H, Zu C, Su Y-S. Rechargeable lithium-sulfur batteries. *Chem Rev*. 2014;114:11751-11787.
88. Xu Y, Wen Y, Zhu Y, et al. Confined sulfur in microporous carbon renders superior cycling stability in Li/S batteries. *Adv Funct Mater*. 2015;25:4312-4320.
89. Li Z, Jiang Y, Yuan L, et al. A highly ordered meso@microporous carbon-supported sulfur@smaller sulfur core-shell structured cathode for Li-S batteries. *ACS Nano*. 2014;8:9295-9303.
90. Wang W, Cao Z, Elia GA, et al. Recognizing the mechanism of sulfurized polyacrylonitrile cathode materials for Li-S batteries and beyond in Al-S batteries. *ACS Energy Lett*. 2018;3:2899-2907.
91. Yang Y, Zheng G, Cui Y. A membrane-free lithium/polysulfide semi-liquid battery for large-scale energy storage. *Energy Environ Sci*. 2013;6:1552-1558.
92. Fu Y, Su YS, Manthiram A. Highly reversible lithium/dissolved polysulfide batteries with carbon nanotube electrodes. *Angew Chem Int Ed*. 2013;52:6930-6935.
93. Guo J, Yang Z, Yu Y, Abruña HD, Archer LA. Lithium-sulfur battery cathode enabled by lithium-nitrile interaction. *J Am Chem Soc*. 2013;135:763-767.
94. Demir-Cakan R, Morcrette M, Guéguen A, Dedryvère R, Tarascon J-M. Li-S batteries: simple approaches for superior performance. *Energy Environ Sci*. 2013;6:176-182.
95. Gao H, Zhou T, Zheng Y, et al. CoS quantum dot nanoclusters for high energy potassium ion batteries. *Adv Funct Mater*. 2017;27:1702634.
96. Cao B, Zhang Q, Liu H, et al. Graphitic carbon nanocage as a stable and high power anode for potassium-ion batteries. *Adv Energy Mater*. 2018;8:1801149.
97. Zhang Q, Wang Z, Zhang S, Zhou T, Mao J, Guo Z. Cathode materials for potassium-ion batteries: current status and perspective. *Electrochem Energy Rev*. 2018;1:625-658.
98. Zhang Q, Didier C, Pang WK, et al. Structural insight into layer gliding and lattice distortion in layered manganese oxide electrodes for potassium-ion batteries. *Adv Energy Mater*. 2019;9:1900568.
99. Xiao N, McCulloch WD, Wu Y. Reversible dendrite-free potassium plating and stripping electrochemistry for potassium secondary batteries. *J Am Chem Soc*. 2017;139:9475-9478.
100. Xue L, Gao H, Zhou W, et al. Liquid K-Na alloy anode enables dendrite-free potassium batteries. *Adv Mater*. 2016;28:9608-9612.
101. Zhang W, Wu Z, Zhang J, et al. Unraveling the effect of salt chemistry on long-durability high-phosphorus-concentration anode for potassium ion batteries. *Nano Energy*. 2018;53:967-974.
102. Ji B, Zhang F, Song X, Tang Y. A novel potassium-ion-based dual-ion battery. *Adv Mater*. 2017;29:1700519.
103. Xu W, Wang J, Ding F, et al. Lithium metal anodes for rechargeable batteries. *Energy Environ Sci*. 2014;7:513-537.
104. Gu Y, Wang W-W, Li Y-J, et al. Designable ultra-smooth ultra-thin solid-electrolyte interphases of three alkali metal anodes. *Nat Commun*. 2018;9:1-9.
105. Wang H, Yu D, Kuang C, et al. Alkali metal anodes for rechargeable batteries. *Chemistry*. 2019;5:313-338.
106. Bhargav A, He J, Gupta A, Manthiram A. Lithium-sulfur batteries: attaining the critical metrics. *Joule*. 2020;4:285-291.
107. Shi S, Lu P, Liu Z, et al. Direct calculation of Li-ion transport in the solid electrolyte interphase. *J Am Chem Soc*. 2012;134:15476-15487.
108. Hosaka T, Muratsubaki S, Kubota K, Onuma H, Komaba S. Potassium metal as reliable reference electrodes of non-aqueous potassium cells. *J Phys Chem Lett*. 2019;10:3296-3300.
109. Hundekar P, Basu S, Fan X, et al. In situ healing of dendrites in a potassium metal battery. *Proc Natl Acad Sci*. 2020;117:5588-5594.
110. Wang H, Hu J, Dong J, et al. Artificial solid-electrolyte interphase enabled high-capacity and stable cycling potassium metal batteries. *Adv Energy Mater*. 2019;9:1902697.
111. Qin L, Lei Y, Wang H, et al. Capillary encapsulation of metallic potassium in aligned carbon nanotubes for use as stable potassium metal anodes. *Adv Energy Mater*. 2019;9:1901427.
112. Yamada Y, Wang J, Ko S, Watanabe E, Yamada A. Advances and issues in developing salt-concentrated battery electrolytes. *Nat Energy*. 2019;4:269-280.
113. Yamada Y, Furukawa K, Sodeyama K, et al. Unusual stability of acetonitrile-based superconcentrated electrolytes for fast-charging lithium-ion batteries. *J Am Chem Soc*. 2014;136:5039-5046.
114. Li L, Basu S, Wang Y, et al. Self-heating-induced healing of lithium dendrites. *Science*. 2018;359:1513-1516.
115. Hundekar P, Basu S, Pan J, et al. Exploiting self-heat in a lithium metal battery for dendrite healing. *Energy Storage Mater*. 2019;20:291-298.
116. Zhang H, Liao X, Guan Y, et al. Lithiophilic-lithiophobic gradient interfacial layer for a highly stable lithium metal anode. *Nat Commun*. 2018;9:1-11.
117. Kim MS, Ryu J-H, Lim YR, et al. Langmuir-Blodgett artificial solid-electrolyte interphases for practical lithium metal batteries. *Nat Energy*. 2018;3:889-898.

118. Huang C, Xiao J, Shao Y, et al. Manipulating surface reactions in lithium-sulphur batteries using hybrid anode structures. *Nat Commun*. 2014;5:1-8.
119. Shi P, Li T, Zhang R, et al. Lithiophilic LiC_6 layers on carbon hosts enabling stable Li metal anode in working batteries. *Adv Mater*. 2019;31:1807131.
120. Lin D, Liu Y, Liang Z, et al. Layered reduced graphene oxide with nanoscale interlayer gaps as a stable host for lithium metal anodes. *Nat Nanotechnol*. 2016;11:626-632.
121. Zhang R, Chen X, Shen X, et al. Coralloid carbon fiber-based composite lithium anode for robust lithium metal batteries. *Joule*. 2018;2:764-777.
122. Wu H, Zhang Y, Deng Y, et al. A lightweight carbon nanofiber-based 3D structured matrix with high nitrogen-doping level for lithium metal anodes. *Sci China Mater*. 2019;62:87-94.
123. Chen X, Chen X-R, Hou T-Z, et al. Lithiophilicity chemistry of heteroatom-doped carbon to guide uniform lithium nucleation in lithium metal anodes. *Sci Adv*. 2019;5:eaau7728.
124. Lu L-L, Zhang Y, Pan Z, Yao H-B, Zhou F, Yu S-H. Lithiophilic Cu-Ni core-shell nanowire network as a stable host for improving lithium anode performance. *Energy Storage Mater*. 2017;9:31-38.
125. Yu W, Lau KC, Lei Y, et al. Dendrite-free potassium-oxygen battery based on a liquid alloy anode. *ACS Appl Mater Interfaces*. 2017;9:31871-31878.
126. Zhang L, Xia X, Zhong Y, et al. Exploring self-healing liquid Na-K alloy for dendrite-free electrochemical energy storage. *Adv Mater*. 2018;30:1804011.
127. Ding Y, Guo X, Qian Y, et al. A liquid-metal-enabled versatile organic alkali-ion battery. *Adv Mater*. 2019;31:1806956.
128. Yu J, Hu Y-S, Pan F, et al. A class of liquid anode for rechargeable batteries with ultralong cycle life. *Nat Commun*. 2017;8:1-7.
129. Cong G, Wang W, Lai N-C, Liang Z, Lu Y-C. A high-rate and long-life organic-oxygen battery. *Nat Mater*. 2019;18:390-396.
130. Xiao Z, Zhou B, Wang J, et al. PEO-based electrolytes blended with star polymers with precisely imprinted polymeric pseudo-crown ether cavities for alkali metal ion batteries. *J Membr Sci*. 2019;576:182-189.
131. Gao H, Xue L, Xin S, Goodenough JB. A high-energy-density potassium battery with a polymer-gel electrolyte and a polyaniline cathode. *Angew Chem Int Ed*. 2018;57:5449-5453.
132. Yuan H, Li H, Zhang T, et al. A $K_2Fe_4O_7$ superionic conductor for all-solid-state potassium metal batteries. *J Mater Chem A*. 2018;6:8413-8418.
133. Li X, Liang J, Luo J, et al. High-performance Li-SeS_x all-solid-state lithium batteries. *Adv Mater*. 2019;31:1808100.
134. Abouimrane A, Dambournet D, Chapman KW, Chupas PJ, Weng W, Amine K. A new class of lithium and sodium rechargeable batteries based on selenium and selenium-sulfur as a positive electrode. *J Am Chem Soc*. 2012;134:4505-4508.
135. Liu Y, Tai Z, Zhang Q, et al. A new energy storage system: rechargeable potassium-selenium battery. *Nano Energy*. 2017;35:36-43.
136. Zheng J, Tian J, Wu D, et al. Lewis acid-base interactions between polysulfides and metal organic framework in lithium sulfur batteries. *Nano Lett*. 2014;14:2345-2352.
137. Pang Q, Liang X, Kwok CY, Nazar LF. Advances in lithium-sulfur batteries based on multifunctional cathodes and electrolytes. *Nat Energy*. 2016;1:1-11.
138. Tao Y, Wei Y, Liu Y, et al. Kinetically-enhanced polysulfide redox reactions by Nb_2O_5 nanocrystals for high-rate lithium-sulfur battery. *Energy Environ Sci*. 2016;9:3230-3239.
139. Al Salem H, Babu G, Rao CV, LMR A. Electrocatalytic polysulfide traps for controlling redox shuttle process of Li-S batteries. *J Am Chem Soc*. 2015;137:11542-11545.
140. Zhang J, Hu H, Li Z, Lou XW. Double-shelled nanocages with cobalt hydroxide inner shell and layered double hydroxides outer shell as high-efficiency polysulfide mediator for lithium-sulfur batteries. *Angew Chem Int Ed*. 2016;55:3982-3986.
141. Wang Z, Dong Y, Li H, et al. Enhancing lithium-sulphur battery performance by strongly binding the discharge products on amino-functionalized reduced graphene oxide. *Nat Commun*. 2014;5:1-8.
142. Zhang C, Wu HB, Yuan C, Guo Z, Lou XW. Confining sulfur in double-shelled hollow carbon spheres for lithium-sulfur batteries. *Angew Chem Int Ed*. 2012;51:9592-9595.
143. Zhang J, Li Z, Chen Y, Gao S, Lou XW. Nickel-iron layered double hydroxide hollow polyhedrons as a superior sulfur host for lithium-sulfur batteries. *Angew Chem Int Ed*. 2018;57:10944-10948.
144. Zhang Y, Katayama Y, Tatara R, et al. Revealing electrolyte oxidation via carbonate dehydrogenation on Ni-based oxides in Li-ion batteries by in situ Fourier transform infrared spectroscopy. *Energy Environ Sci*. 2020;13:183–199.
145. Zhang L, Qian T, Zhu X, et al. In situ optical spectroscopy characterization for optimal design of lithium-sulfur batteries. *Chem Soc Rev*. 2019;48:5432-5453.
146. Fan Z, Zhang L, Baumann D, et al. In situ transmission electron microscopy for energy materials and devices. *Adv Mater*. 2019;31:1900608.
147. Liang G, Wu Z, Didier C, et al. A long cycle-life high-voltage spinel lithium-ion battery electrode achieved by site-selective doping. *Angew Chem Int Ed*. 2020.59 2–11.
148. Liang G, Didier C, Guo Z, Pang WK, Peterson VK. Understanding rechargeable battery function using in operando neutron powder diffraction. *Adv Mater*. 2019;1904528.32 1904528
149. Wu Z, Liang G, Pang WK, et al. Coupling topological insulator $SnSb_2Te_4$ nanodots with highly doped graphene for high-rate energy storage. *Adv Mater*. 2020;32:1905632.
150. Zachman MJ, Tu Z, Choudhury S, Archer LA, Kourkoutis LF. Cryo-STEM mapping of solid-liquid interfaces and dendrites in lithium-metal batteries. *Nature*. 2018;560:345-349.
151. Li Y, Li Y, Cui Y. Looking cool. *Nat Energy*. 2018;3:1023-1024.
152. Yan Y, Yin Y-X, Xin S, Su J, Guo Y-G, Wan L-J. High-safety lithium-sulfur battery with prelithiated Si/C anode and ionic liquid electrolyte. *Electrochim Acta*. 2013;91:58-61.
153. Park J-W, Ueno K, Tachikawa N, Dokko K, Watanabe M. Ionic liquid electrolytes for lithium-sulfur batteries. *J Phys Chem C*. 2013;117:20531-20541.
154. Zhang S, Ueno K, Dokko K, Watanabe M. Recent advances in electrolytes for lithium-sulfur batteries. *Adv Energy Mater*. 2015;5:28.

155. Liu S, Mao J, Zhang Q, et al. An intrinsically non-flammable electrolyte for high-performance potassium batteries. *Angew Chem Int Ed*. 2020;59:3638-3644.
156. Chung S-H, Manthiram A. Designing lithium-sulfur cells with practically necessary parameters. *Joule*. 2018;2:710-724.
157. Agostini M, Hwang JY, Kim HM, et al. Minimizing the electrolyte volume in Li-S batteries: a step forward to high gravimetric energy density. *Adv Energy Mater*. 2018;8:1801560.

AUTHOR BIOGRAPHIES

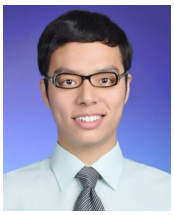

Dr Xinyu Zhao received his PhD from the Shanghai Institute of Ceramics, Chinese Academy of Sciences in 2014. He continued his career as a postdoctoral research fellow at the Singapore University of Technology and Design. He is currently a postdoctoral research fellow at Shenzhen University and a visiting fellow at the University of Wollongong. His expertise lies mainly in the design and controlled synthesis of functional inorganic nanomaterials and polymer-inorganic nanocomposites. His current research includes the synthesis and application of functional nanomaterials for energy devices.

Dr Yan Lu is currently an ARC DECRA Fellow at the University of Wollongong, Australia. She obtained her PhD degree from Shanghai Institute of Ceramics, Chinese Academy of Sciences in 2014, under the supervision of Prof Zhaoyin Wen. She was a postdoctoral research fellow at Dr Eileen Fong's group (2014-2016), Prof Xiongwen (David) Lou's group (2016-2018), and Prof Rong Xu's group (2018) at Nanyang Technological University, Singapore. After being awarded the ARC DECRA fellowship, Dr Lu joined Prof Zaiping Guo's group as a research staff. Her research focuses on the rational design and controllable fabrication of complex nanostructured functional materials and their applications for rechargeable batteries and efficient electrocatalysis.

Dr Renheng Wang received his PhD degree in Metallurgical Engineering from Central South University (CSU) in 2015. From January 2016 to October 2018, he worked as a postdoctoral follow at Shenzhen University and Nanyang Technological University. He is now a researcher in the College of Physics and Optoelectronic Engineering, Shenzhen University. His research is focused on the synthesis and application of nanomaterials and composites for clean energy storage, such as high-power/high-energy lithium ion batteries.

Prof Zaiping Guo is currently a Distinguished Professor at the University of Wollongong, Australia. She received her PhD in Materials Engineering from the University of Wollongong in December 2003. After her Australian Postdoctoral (APD) fellowship in the Institute for Superconducting & Electronic Materials, she joined the Faculty of Engineering and Information Sciences, University of Wollongong as a Lecturer in 2008, was promoted to Professor in 2012, and then Senior Professor in 2013. Her current research interests are mainly focused on energy storage applications, such as lithium ion batteries, sodium ion batteries, potassium ion batteries, and hydrogen storage, as well as electrochemistry characterization and computer modeling.

How to cite this article: Zhao X, Lu Y, Qian Z, Wang R, Guo Z. Potassium-sulfur batteries: Status and perspectives. *EcoMat*. 2020;2:e12038. https://doi.org/10.1002/eom2.12038